

Empowering COVID-19 Detection: Optimizing Performance Through Fine-Tuned EfficientNet Deep Learning Architecture

Md. Alamin Talukder^{*a}, Md. Abu Layek^a, Mohsin Kazi^b, Md Ashraf Uddin^c, Sunil Aryal^c

^aDepartment of Computer Science and Engineering, Jagannath University, Dhaka, Bangladesh

^bDepartment of Pharmaceutics, College of Pharmacy, King Saud University, Riyadh, Saudi Arabia

^cSchool of Information Technology, Deakin University, Waurn Ponds Campus, Geelong, Australia

Abstract

The worldwide COVID-19 pandemic has profoundly influenced the health and everyday experiences of individuals across the planet. It is a highly contagious respiratory disease requiring early and accurate detection to curb its rapid transmission. Initial testing methods primarily revolved around identifying the genetic composition of the coronavirus, exhibiting a relatively low detection rate and requiring a time-intensive procedure. To address this challenge, experts have suggested using radiological imagery, particularly chest X-rays, as a valuable approach within the diagnostic protocol. This study investigates the potential of leveraging radiographic imaging (X-rays) with deep learning algorithms to swiftly and precisely identify COVID-19 patients. The proposed approach elevates the detection accuracy by fine-tuning with appropriate layers on various established transfer learning models. The experimentation was conducted on a COVID-19 X-ray dataset containing 2000 images. The accuracy rates achieved were impressive of 99.55%, 97.32%, 99.11%, 99.55%, 99.11% and 100% for Xception, InceptionResNetV2, ResNet50, ResNet50V2, EfficientNetB0 and EfficientNetB4 respectively. The fine-tuned EfficientNetB4 achieved an excellent accuracy score, showcasing its potential as a robust COVID-19 detection model. Furthermore, EfficientNetB4 excelled in identifying Lung disease using Chest X-ray dataset containing 4,350 Images, achieving remarkable performance with an accuracy of 99.17%, precision of 99.13%, recall of 99.16%, and f1-score of 99.14%. These results highlight the promise of fine-tuned transfer learning for efficient lung detection through medical imaging, especially with X-ray images. This research offers radiologists an effective means of aiding rapid and precise COVID-19 diagnosis and contributes valuable assistance for healthcare professionals in accurately identifying affected patients.

Keywords: COVID-19; Diagnosis; Deep Learning; Transfer Learning; X-Ray Image; EfficientNet

1. Introduction

The COVID-19 pandemic had a profound global impact, beginning with a significant outbreak in December 2019 in Wuhan, China. This infectious and unconventional form of pneumonia, caused by the zoonotic coronavirus known as SARS-CoV-2, rapidly disseminated worldwide. By mid-2022, approximately 600 million confirmed cases and a substantial number of deaths had been reported, as indicated by data from Worldometer Batagelj et al. (2021); Eyiokur et al. (2022). COVID-19 is an infectious respiratory disease triggered by exposure to the virus,

*Corresponding author: Md. Alamin Talukder

Email addresses: alamintalukder.cse.jnu@gmail.com (Md. Alamin Talukder*), layek@cse.jnu.ac.bd (Md. Abu Layek), mkazi@ksu.edu.sa (Mohsin Kazi), ashraf.uddin@deakin.edu.au (Md Ashraf Uddin), sunil.aryal@deakin.edu.au (Sunil Aryal)

impacting the respiratory system. Initial signs, like cold, fever, and breathlessness, can emerge from day two to fourteen post-exposure. The impact on an individual varies based on immune strength and disease intensity. The virus can be transmissible up to two days before symptom onset and for 10 to 20 days afterward Subramanian et al. (2023).

The global impact of the COVID-19 pandemic has been staggering, with infection statistics reflecting its widespread reach. As of the latest available data, there have been more than 474 million confirmed cases of COVID-19 reported worldwide, underscoring the scale of this global health crisis Filfilan et al. (2023). The virus has demonstrated a remarkable ability to transcend borders, affecting individuals in nearly every corner of the world. The severity of its impact is further highlighted by the tragic loss of around 6 million lives attributed to the disease Nemati et al. (2023). These statistics serve as a stark reminder of the urgent need for comprehensive strategies to curb the spread of the virus, protect vulnerable populations, and ensure effective healthcare responses Alamri et al. (2023).

Deep learning (DL) is a branch of machine learning that has shown its effectiveness in many application areas Talukder et al. (2023b). DL models are basically multilayered architectures of neural networks capable of extracting complex features from the image and have played important roles in image classifications and disease detection specially in the biomedical field Talukder et al. (2022b, 2023a); Sharmin et al. (2023). For example, it can be useful to detect diabetes detection, predicting pneumonia or related diseases by analyzing CT scans or human brain tumors using histopathology images Talukder et al. (2023b); Ahamed et al. (2021, 2023); Xue et al. (2023); Motta et al. (2023). Thus, deep learning has grown enormous interest in computer-aided diagnosis systems to improve the classification detection performance in a very short period of time Zysman et al. (2023); Afif et al. (2023).

Transfer learning models have emerged as a powerful tool for COVID-19 detection Kathamuthu et al. (2023); Agrawal et al. (2023); Rana et al. (2023); Islam et al. (2023). These models showcase exceptional potential in identifying COVID-19 cases from X-ray images by leveraging pre-trained neural networks on extensive datasets SUBASI et al. (2023). Their ability to learn rich features from diverse image sets equips them to generalize effectively, even in the presence of limited COVID-19 data. This approach aids in overcoming data scarcity challenges, enabling quicker and more accurate diagnosis. Through fine-tuning and retraining, transfer learning models can adapt to the nuances of COVID-19 patterns, contributing significantly to the ongoing efforts in combatting the pandemic Motta et al. (2023); Zheng et al. (2023).

COVID-19's multifaceted implications, ranging from the spread of infection to the strain on healthcare systems, call for innovative approaches that address these challenges comprehensively Elbeltagi et al. (2023). Traditional testing methods have shown limitations, such as delays in results and the potential for transmission during testing procedures. Deep learning, with its ability to discern intricate patterns and relationships in complex data, has the potential to revolutionize COVID-19 detection Duong et al. (2023). The process of fine-tuning deep learning models for this purpose is particularly captivating, as it involves customizing pre-trained models to specific datasets, thereby refining their capabilities to accurately identify COVID-19 cases.

In the realm of COVID-19 detection, traditional methods have faced several challenges that hinder their effectiveness. Currently, three primary methods are employed for diagnosing COVID-19: molecular, antigen, and antibody testing Brooks and Das (2020). However, these methods come with limitations that impact their suitability

ity, particularly in resource-constrained settings. Antigen testing offers rapid results, but the affordability of test kits remains a concern, especially for developing countries Peeling et al. (2020). Meanwhile, the accuracy of RT-PCR tests is influenced by various factors, such as the timing of sample collection, type of sample, storage conditions, handling, and processing. This complexity can lead to false negatives if not executed meticulously Ahmed et al. (2022). Moreover, traditional testing methods can only detect active infections, leaving a gap in identifying past infections. A critical issue arises from the potential for false negatives due to improper sample collection or testing timing. An individual tested too soon after exposure might yield a negative result, as the virus's presence might not be detectable yet. Conversely, testing too late into the infection cycle can also lead to false negatives as the viral load decreases. These challenges collectively highlight the limitations of conventional diagnostic approaches. One of the conventional clinical tools used for preliminary respiratory investigation is the chest x-ray (CXR), which is cost-effective and easily accessible. However, its effective utilization requires skilled radiologists to accurately identify COVID-19 patients. Overcoming these limitations calls for innovative solutions that can provide accurate and timely diagnoses.

Deep learning offers a transformative approach to tackling these challenges. Through harnessing the capabilities of neural networks and extensive datasets, deep learning models can significantly augment the accuracy of COVID-19 detection, effectively surpassing the limitations associated with conventional methods Elbeltagi et al. (2023). With the potential to furnish more precise outcomes in shorter timeframes, deep learning holds the potential to revolutionize the realm of diagnostics and contribute to more efficacious pandemic management Li et al. (2023a). In response to the shortcomings of PCR-based testing, a shift towards radiographic imaging has gained substantial momentum as a reliable and accurate means of early-stage COVID-19 detection Panwar et al. (2020); Karakanis and Leontidis (2021); Muhammad et al. (2022). An instance of this paradigm is found in the work of Panwar et al. (2020), who introduced a CNN-based detection approach utilizing binary classification with chest X-ray images, achieving an overall accuracy of approximately 88.10%. Meanwhile, Hemdan et al. (2020) explored various deep learning algorithms for COVID-19 image classification, with DenseNet exhibiting the highest accuracy at 90%. By deploying AlexNet, ResNet18, DenseNet201, and SqueezeNet on a dataset containing 1579 normal, 1485 viral pneumonia, and 423 COVID-19 positive X-ray images, Chowdhury et al. (2020) achieved a maximum accuracy of 97.94%. Further exploration of deep learning models in COVID-19 detection Nigam et al. (2021) revealed the varied performance of DenseNet121, VGG16, Xception, EfficientNet, and NASNet, with EfficientNet leading with an accuracy of 93.48%. Similarly, Kogilavani et al. (2022) evaluated a range of models, with VGG16 achieving an accuracy of 97.68%, DenseNet121 reaching 97.53%, MobileNet attaining 96.38%, NASNet scoring 89.51%, Xception achieving 92.47%, and EfficientNet yielding an accuracy of 80.19%. This showcases the remarkable potential of deep learning in significantly enhancing COVID-19 detection accuracy, thereby contributing to more effective healthcare strategies during the ongoing pandemic.

While the existing solutions demonstrate the capability to reliably detect COVID-19, the accuracy rate of current research remains below the desired level. Addressing this challenge, the realm of AI-based COVID-19 detection systems has garnered significant research attention. Numerous researchers have posed the following pivotal research inquiries, accompanied by their proposed methodologies, to address the aforementioned concerns effectively:

1. How can an optimal automated COVID detection model be developed to enhance accuracy and overcome the

limitations observed in current solutions?

2. In what manner can this novel detection model be seamlessly integrated with COVID-19 datasets, ensuring seamless compatibility and maximizing its potential to achieve precise prediction?
3. How can the existing models be fine-tuned and optimized to attain notably elevated levels of accuracy, thus bolstering the reliability and effectiveness of COVID-19 detection?

These research inquiries encapsulate the core objectives of tackling accuracy challenges in contemporary COVID-19 detection methods through innovative AI-driven approaches. By concentrating on the conception, application, and refinement of advanced detection models, researchers aim to propel the field toward more dependable and accurate diagnostic outcomes, significantly influencing the management of the ongoing pandemic.

The contributions of this research encompass several significant aspects that collectively enhance the field of COVID-19 detection and diagnosis:

- We presented a novel approach that leverages the power of deep learning to accurately identify COVID-19 manifestations in medical images. Our model stands as a testament to the potential of integrating cutting-edge technology with medical diagnostics, offering a promising solution in the battle against the pandemic.
- To harness the full potential of transfer learning, we embarked on a rigorous fine-tuning process. By meticulously modifying an existing transfer learning model and introducing additional layers, we optimized its applicability to our proposed approach. This meticulous tailoring serves as a testament to our commitment to achieving optimal performance in COVID-19 detection.
- We meticulously evaluated our fine-tuned models using a plethora of performance metrics, ensuring that the chosen model excels in terms of accuracy, precision, recall, f1-score, and beyond. This exhaustive evaluation process is a testament to our dedication to reducing loss of life through accurate and swift COVID-19 detection.
- The culmination of our contributions is a fine-tuned DL model with immense potential for real-world impact. By offering accurate and rapid COVID-19 detection, our research has the potential to revolutionize medical diagnostics and contribute significantly to global efforts in managing and combating the pandemic.

Collectively, our contributions reflect a harmonious blend of technological innovation, rigorous fine-tuning, and comprehensive evaluation. This research represents a significant stride towards refining COVID-19 detection methods and advancing the landscape of healthcare diagnostics.

The rest of the paper is organized as follows. In section 2, we review the related literature for covid-19 detection. In Section 3, we describe our proposed methodology and various transfer learning algorithms. Experimental results are presented in Section 4. Then, in Section 5, we present the results analysis and discussion and Finally, in Section 6, we conclude the paper with the future enhancement of this study.

2. Literature Review

In the wake of the initial outbreak of COVID-19 infections, numerous researchers have explored the application of deep learning techniques to address the challenges of COVID-19 detection. This literature review categorizes previous research based on different Deep-Learning strategies and datasets employed in experiments.

2.1. COVID-19 Detection using Transfer Learning Model on X-Rays Image

Agrawal et al. (2023) conducted a comprehensive evaluation of classic models (VGG19, ResNet50, MobileNetV2, InceptionV3, Xception, DenseNet121) and specialized models (DarkCOVIDNet, COVID-Net) on covid-19 dataset. The study demonstrated that ResNet50 exhibited the best performance. Furthermore, a simple modification to the ResNet50 model achieved impressive binary classification accuracy (99.20%) and multi-class classification accuracy (86.13%), solidifying its effectiveness for COVID-19 detection and differentiation from pneumonia. Model explanations using LIME and Grad-CAM highlighted its generalization capacity, particularly in identifying COVID-19-concentrated lung regions. The proposed model is designed for free deployment.

Asif et al. (2023) introduced a CNN model employing deep transfer learning with six distinct pre-trained architectures: VGG16, DenseNet201, MobileNetV2, ResNet50, Xception, and EfficientNetB0. They utilized a dataset of 3886 Chest-X-Ray, consisting of 1200 COVID-19 cases, 1341 healthy cases, and 1345 viral pneumonia cases, to assess the CNN model's effectiveness. A comparative analysis of the CNN models across three chest X-ray classes aimed to determine the most suitable model. The results highlighted the VGG16-based CNN model as capable of accurately diagnosing COVID-19 patients, achieving a 97.84% accuracy, 97.90% precision, 97.89% sensitivity, and 97.89% F1-score. The evaluation demonstrated that this model outperformed other CNN models, making it a favorable choice for COVID-19 classification and assisting healthcare professionals in enhancing patient screening during the pandemic.

Madhavan et al. (2023) introduced a framework named Res-CovNet, employing transfer learning with ResNet-50 as a pre-trained model extended by classification layers. The research used a dataset of X-ray images from reliable repositories, covering normal, bacterial pneumonia, viral pneumonia, and COVID-19 cases, totaling approximately 5856 images. The model achieved a remarkable accuracy of 98.4% in distinguishing COVID-19 from normal cases, and a 96.2% accuracy in identifying COVID-19 across all case categories.

2.2. COVID-19 Detection using Ensemble Transfer Learning Model on X-Rays Image

Kumar et al. (2023) introduced an ensemble model for early detection of COVID-19 infection using chest X-ray images. The approach leverages transfer learning by integrating pre-trained models like EfficientNet, GoogLeNet, and XceptionNet. This ensemble model categorizes patients into COVID-19, pneumonia, tuberculosis, or healthy groups, demonstrating improved generalization for both binary and multiclass COVID-19 datasets. The model's performance surpasses existing state-of-the-art methods, as validated through comparative analysis on two prominent datasets.

2.3. COVID-19 Detection using Trained Output-based Transfer Learning Model on X-Rays Image

Kumar and Mallik (2023) proposed a novel Trained Output-based Transfer Learning (TOTL) approach for COVID-19 detection from chest X-rays. The method involved preprocessing images using denoising, contrasting, and segmentation techniques. These processed images were then utilized to fine-tune several pre-trained transfer learning models, including InceptionV3, InceptionResNetV2, Xception, MobileNet, ResNet50, ResNet50V2, VGG16, and VGG19. The model's outputs were further trained using a deep neural network architecture to enhance performance and combine their strengths. Testing on various COVID-19 chest X-ray datasets and comparison with other models and methods revealed the efficiency and effectiveness of the proposed approach.

2.4. COVID-19 Detection using Self-Supervised Transfer Learning Model on X-Rays Image

Li et al. (2023b) presented a novel self-supervised transfer learning approach for detecting COVID-19 in chest X-ray (CXR) images. The proposed method was compared with six self-supervised learning methods and six pre-trained deep convolutional neural networks on a comprehensive COVID-19 CXR dataset. The results indicated that the proposed method achieved a harmonic mean score of 0.985, an AUC of 0.999, and a four-class accuracy of 95.3%. The research demonstrated that leveraging transfer learning knowledge from natural images enhances self-supervised learning of CXR images and improves representation learning for COVID-19 detection. The potential of this approach to decrease infections among radiologists and healthcare providers is noteworthy.

2.5. COVID-19 Detection using Feature Extraction based Transfer Learning Model on X-Rays Image

The MMF-DTL model introduced by Reddy et al. (2023), consists of three main steps: pre-processing, feature extraction, and classification. It employs three deep learning models (VGG16, Inception v3, and ResNet 50) for extracting features. To enhance detection efficiency, the model combines these three approaches using decision-based multimodal fusion. This fusion of deep learning models contributes to a better detection rate. Ultimately, a softmax classifier is utilized to classify test images into six categories. The model's performance is extensively evaluated on the Chest-X-Ray dataset, demonstrating its effectiveness in diagnosing COVID-19 through radiological images. The fusion model achieves an average accuracy of 98.80% and an F-score of 93.26%.

2.6. COVID-19 Detection using Explainable Artificial Intelligence-based Transfer Learning Model on X-Rays Image

Sarp et al. (2023) introduced a model for the detection and interpretation of COVID-19-positive chest X-ray (CXR) images, employing Explainable Artificial Intelligence (XAI) techniques. The impact of COVID-19-positive CXR images was analyzed through heatmaps. The approach utilized transfer learning and data augmentation methods to expedite and improve model training, with additional enhancement from lung segmentation. A comparison of pre-trained networks highlighted the ResNet model as achieving the highest classification performance, with an F1-Score of 98

2.7. COVID-19 Detection using Transfer Learning Model on CT images

Choudhary et al. (2023) aimed to identify COVID-19 presence in CT-scan images using a specialized weights-only transfer learning technique, specifically tailored for devices with limited runtime resources. This method involved optimizing pre-trained models for compatibility with point-of-care devices through the selective pruning of less essential weight parameters. The study focused on assessing the approach using two widely recognized models: VGG16 and ResNet34. The experimental results showcased that the pruned ResNet34 model achieved notable performance metrics, including a 95.47% accuracy rate, 92.16% sensitivity, 95.67% F-score, and 99.42% specificity. Moreover, the pruned model demonstrated efficiency improvements by utilizing 41.96% fewer FLOPs and having 20.64% fewer weight parameters compared to the unpruned model. These outcomes highlighted the potential of the proposed approach to significantly alleviate the runtime resource demands of resource-intensive models, making them more viable for deployment on point-of-care devices.

Kathamuthu et al. (2023) conducted a deep transfer learning-based CNN approach to detect COVID-19 in chest CT images. The research involved evaluating various models, including VGG16, VGG19, Densenet121, InceptionV3,

Xception, and Resnet50, using metrics such as accuracy, recall, precision, f1-score, loss, and ROC. Among these models, VGG16 exhibited superior performance with an accuracy of 98.00%, outperforming the other models. The study's findings suggested that the proposed model held promise for detecting and monitoring COVID-19, offering potential assistance to healthcare professionals in making informed decisions regarding suitable treatment strategies.

Subramanian et al. (2023) employed transfer learning with three pre-trained deep CNN models (VGG-16, ResNet, and wide ResNet) to detect COVID-19 infection from CT images. However, retraining these models caused a loss of generalization capability on the original datasets. The innovative aspect was incorporating Learning without Forgetting (LwF) with deep CNN architectures to enhance the models' generalization skills on existing and new data. LwF enabled the network to utilize its learning while training on new data, preserving its original abilities. The performance of deep CNN models, combined with LwF, was evaluated on both original images and CT scans of individuals infected with the Delta variant of the SARS-CoV-2 virus. Experimental outcomes demonstrated that the wide ResNet model exhibited superior and effective classification performance among the three fine-tuned CNN models using the LwF technique. It achieved an accuracy of 93.08% for the original dataset and 92.32% for the delta-variant dataset.

2.8. COVID-19 Detection using AI diagnostic tool on Chest-X-Ray Image

Duong et al. (2023) developed a robust expert system capable of detecting COVID-19 from diverse image sources, creating a versatile AI diagnostic tool. The proposed approach was validated using four real-world datasets: two containing chest X-ray (CXR) images with 15,000 and 17,905 images, respectively, and two with lung CT (LCT) images having 2,482 and 411,528 images respectively. Employing a five-fold cross-validation method, the approach demonstrated strong predictive performance across all datasets, consistently achieving accuracy rates exceeding 95.0%. In comparison with existing studies, the approach exhibited substantial and statistically significant performance enhancements.

In conclusion, the literature reflects a proliferation of machine learning and deep learning methods to comprehend and combat the multifaceted challenges posed by COVID-19, spanning detection, diagnosis, prediction, and analysis across diverse data modalities and medical imaging techniques.

3. Proposed Methodology

Our methodology for COVID-19 detection using a Fine-tuned Efficient Deep Learning (DL) model consists of several key stages, as detailed below. Figure 1 illustrates the architecture of the proposed COVID-19 detection model.

Firstly, we collected a comprehensive dataset of COVID-19 X-ray images to serve as the foundation for our experimental setup. Subsequently, we engaged in image preprocessing, ensuring that the collected images were suitably prepared for input into our DL model. In the pursuit of enhancing model robustness, we carried out image augmentation, employing techniques that effectively expanded the diversity of our training dataset. Moreover, we enlisted a selection of deep learning models, which we incorporated into our experimentation framework. Central to our methodology is the fine-tuning process, during which we harnessed a pre-trained convolutional model. Through

this process, we meticulously adapted the model's parameters to align with the unique features relevant to COVID-19 detection. The culmination of our efforts lies in the rigorous evaluation of these fine-tuned models. A range of performance metrics was employed, encompassing accuracy and loss graph, accuracy, precision, recall, F1-score, MAE, MSE and RMSE. The objective was to discern the most adept model for COVID-19 detection.

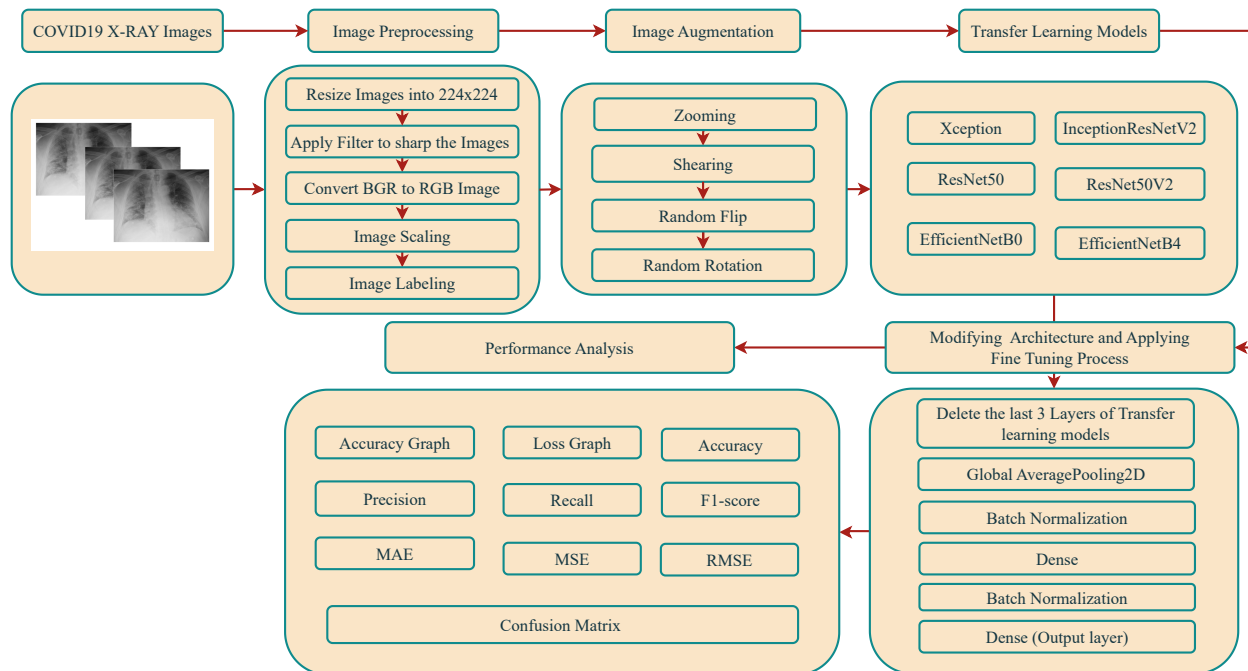


Figure 1: The proposed COVID-19 detection architecture

3.1. Data Collection

For our COVID-19 detection experiment, we utilized two distinct datasets to assess the performance of our fine-tuned model. The first dataset, the COVID-19 X-Ray dataset Talukder et al. (2022a), has been rigorously validated by clinicians and researchers, establishing its credibility. This dataset comprises a diverse collection of X-ray images, encompassing both normal and COVID-19 cases. The images were meticulously sourced from multiple hospitals in Bangladesh. In total, this dataset contains 2,000 images, evenly distributed between normal and COVID-19 cases, with 1,000 images in each category. This balanced distribution provides a solid foundation for model training and evaluation. The dataset's high image quality and sharpness facilitate the effective extraction of critical diagnostic information, essential for accurate COVID-19 detection. By leveraging this dataset, our experiment benefits from the variety and reliability of the included images, contributing to the robustness and accuracy of our proposed COVID-19 detection model. The distribution of this dataset is illustrated in Figure 2(a), where both classes are balanced.

In expansion, we incorporated the "Chest X-Ray Image Dataset," Talukder (2023) which serves as a valuable resource for researchers and healthcare professionals. This dataset comprises a total of 4,350 high-quality images, meticulously sourced from various hospitals in Bangladesh. The dataset is categorized into four distinct classes: Normal (1200 Images): These images represent healthy lung conditions, providing a baseline for comparison. Lung Opacity (1100 Images): This class includes X-ray images featuring lung abnormalities that require further analysis.

Covid (1050 Images): It contains X-ray images from individuals with confirmed or suspected COVID-19 cases, aiding in the early detection and monitoring of the disease. Viral Pneumonia (1000 Images): Images in this category are associated with viral pneumonia cases, contributing to the understanding and identification of this specific lung infection. This dataset adds significant diversity and depth to our experiment, enabling us to assess our fine-tuned model's effectiveness in detecting not only COVID-19 but also a range of other lung diseases. The distribution of this dataset is presented in Figure 2(b), where classes are not balanced.

By utilizing these two datasets, our experiment demonstrates the capability of our fine-tuned model to effectively detect COVID-19 and Lung diseases, thus contributing to the field of medical diagnostics.

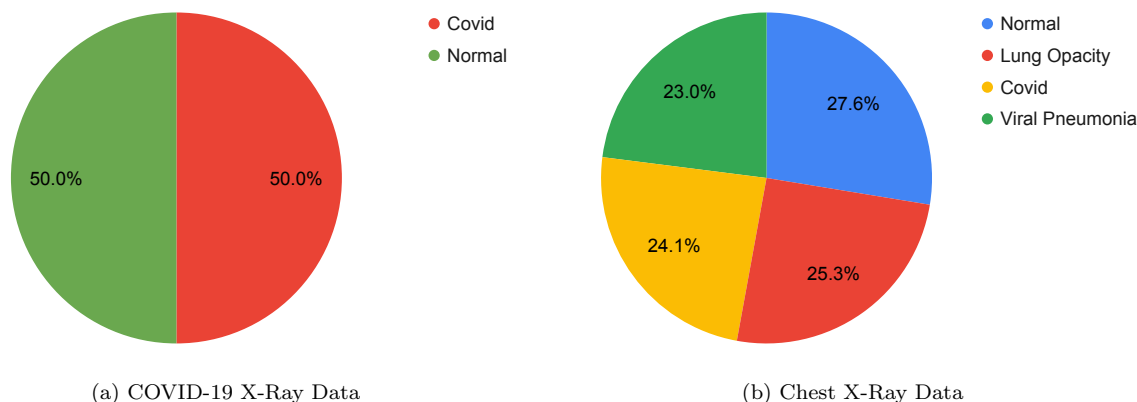


Figure 2: Distribution of COVID-19 and Chest X-Ray Dataset

3.2. Image Preprocessing

The preprocessing of images from the dataset is a critical preparatory phase, essential for enhancing the accuracy and overall performance of our learning module. This phase encompasses a series of operations designed to integrate, clean, normalize, and transform image data.

Figure 3 and Figure 4 visually demonstrate the impact of our preprocessing operations on COVID-19 X-ray and Chest X-Ray Image Datasets, showcasing the transformation from the original state to the preprocessed state. The preprocessing methods detailed in the figure include:

1. **Resizing Images:** To maintain uniform dimensions across all images in the dataset, we resized them to 256x256 pixels. This resizing operation was an essential step to ensure consistency and compatibility with our chosen model.
2. **Applying Filter to Sharpen Image:** We applied image filters to enhance image sharpness and clarity. This procedure aimed to accentuate critical features in the X-ray images while reducing noise, thereby improving the model's ability to extract meaningful information from the data.
3. **Converting BGR to RGB:** Images captured in the BGR (Blue-Green-Red) color space were converted to the RGB (Red-Green-Blue) color space. This conversion ensures color uniformity and facilitates the accurate interpretation of image features.

4. **Image Scaling:** Scaling involves adjusting the intensity values of image pixels to map them to a desired range. This operation standardizes pixel values, promoting better model convergence during the training process.
5. **Image Labeling:** Accurate and consistent image labeling is a fundamental aspect of supervised learning. We ensured that the dataset's images were appropriately labeled, a crucial prerequisite for effective model training.

The purpose of Figure 3 and Figure 4 is to provide a visual representation of these preprocessing steps and their effects on the input images. This illustration serves to make the paper more accessible and comprehensible to readers, allowing them to visually grasp the transformation of raw data into preprocessed data.

Furthermore, it is crucial to note that the necessity of various image preprocessing tasks can vary depending on the dataset, the specific problem at hand, and the characteristics of the deep learning model being employed. While deep learning models have shown remarkable capabilities in handling complex features from raw data, image preprocessing remains relevant for several reasons:

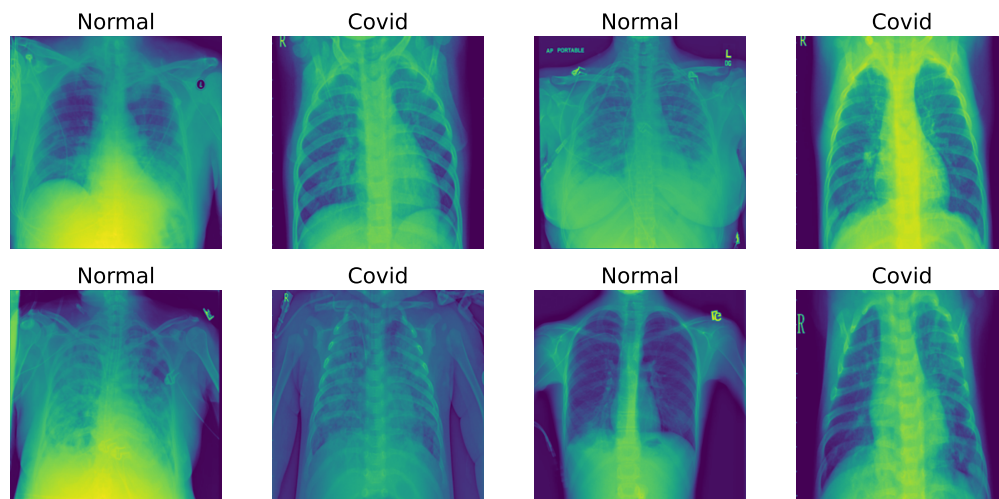
- **Data Quality and Consistency:** Image preprocessing helps ensure that the input data is of high quality, free from noise or artifacts. This is essential to avoid undesirable variations in the training dataset that can affect model performance.
- **Normalization:** Certain preprocessing steps, like image scaling and intensity normalization, assist in standardizing pixel values, which can contribute to better model convergence.
- **Feature Extraction:** Some preprocessing operations, such as image filtering, can enhance the extraction of critical features from images, making it easier for the deep learning model to learn and make accurate predictions.
- **Efficiency:** Appropriate preprocessing can reduce the computational burden and training time of deep learning models, making them more efficient in practice.

In our research, the selected image preprocessing tasks were chosen to improve the overall model performance and the quality of predictions for COVID-19 detection.

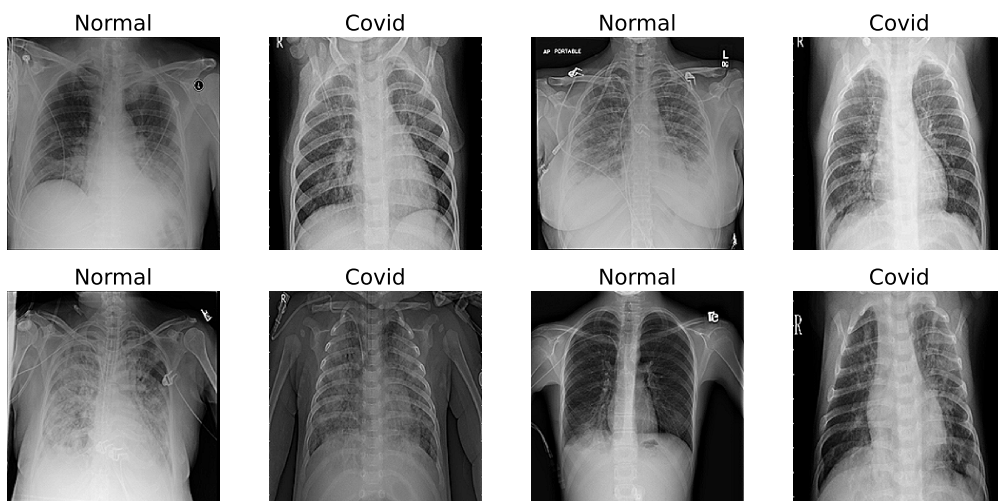
3.3. Image Augmentation

In deep learning, image augmentation is a crucial technique that serves to enhance the robustness and generalization capabilities of models by artificially diversifying the training dataset. This process involves applying a variety of transformations and modifications to the existing images, thus creating new variations while preserving the underlying content. Within our methodology, we have seamlessly integrated the process of image augmentation, a technique meticulously designed to bolster our model's robustness by synthetically diversifying the training dataset. This augmentation process encompasses:

- **Zooming:** Amplifying an image to emphasize specific components, facilitating the model in capturing vital details.



(a) Before Processing



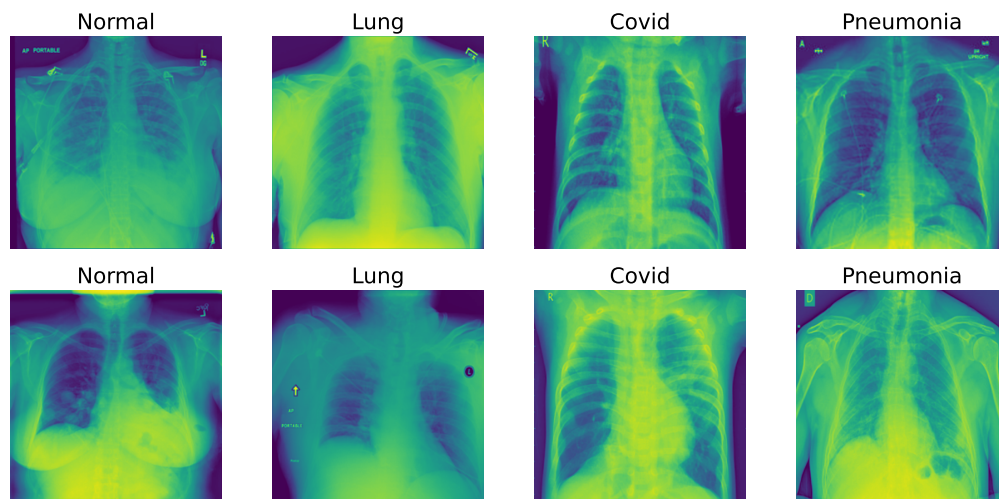
(b) After Processing

Figure 3: Before and After Preprocessing of Covid19 X-Ray dataset

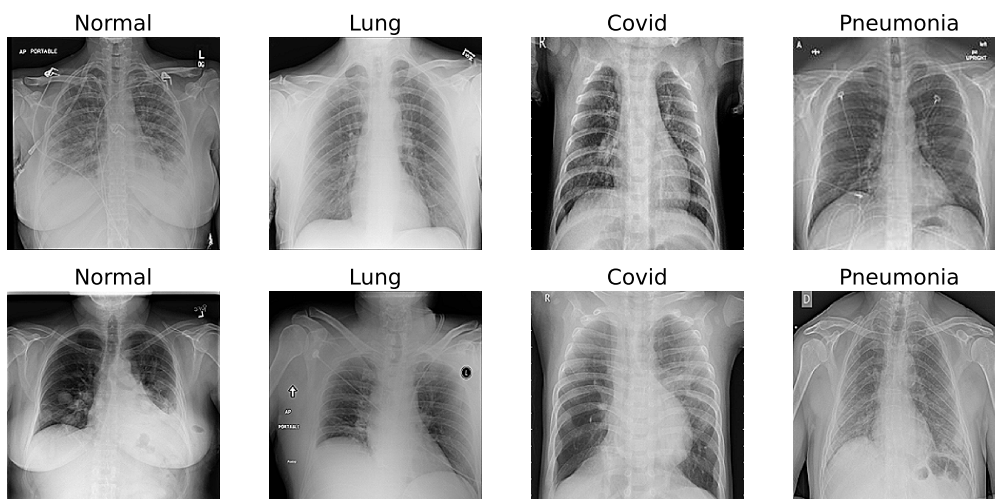
- **Shearing:** Modifying an image along an axis to correct perspective angles and enhance the model's understanding of diverse viewpoints.
- **Random Flipping:** Horizontally flipping images at random to further augment dataset diversity.
- **Random Rotation:** Introducing random rotations to the images, aiding the model in recognizing features from varying orientations.

This image augmentation process unfolds dynamically during the model training phase, occurring on-the-fly as the model is constructed. By incorporating these preprocessing and augmentation techniques, we equip our model to adeptly accommodate variations in image quality, size, and perspective, culminating in a notable enhancement in the accuracy of our COVID-19 detection capabilities.

In our image augmentation process, we assigned equal weightage to the rotation, flip, shearing, and zooming



(a) Before Processing



(b) After Processing

Figure 4: Before and After Preprocessing of Chest X-Ray Dataset

techniques. Our approach aimed to ensure a balanced application of these augmentation operations, with the intent of introducing diversity into the training dataset while avoiding overemphasis on any particular operation.

By giving equal weightage to these techniques, we sought to maintain a well-rounded and representative dataset that captures various aspects of variation and distortion that the model might encounter in real-world scenarios. This balanced approach helps enhance the model's robustness and generalization capabilities, making it better equipped to handle a wide range of input variations.

3.4. Transfer learning Models

The applications of transfer learning in deep learning are multifaceted and have revolutionized the field, offering significant advantages in various domains. Transfer learning, a technique that leverages knowledge from one task to improve performance on another related task, has found particularly robust applications in image classification, natural language processing, and reinforcement learning. In image classification, for instance, pre-trained convolutional

neural networks such as DenseNet, ResNet, and Inception etc have learned a rich hierarchy of features from vast and diverse image datasets. Transfer learning empowers the reuse of these learned features, allowing the development of highly accurate models with substantially reduced data requirements. In natural language processing, models like BERT and GPT-3 have demonstrated the power of transfer learning by pre-training on large text corpora and subsequently fine-tuning for specific language understanding tasks. These models have significantly improved the state of the art in tasks like sentiment analysis, machine translation, and question-answering. Additionally, in reinforcement learning, transfer learning techniques have enabled agents to apply knowledge learned in one environment to perform better in new and unseen environments, reducing the need for extensive exploration and training. Transfer learning's versatility and broad applications continue to drive innovation in artificial intelligence and have become indispensable tools for addressing complex real-world challenges.

The necessity of transfer learning in COVID-19 detection becomes evident when considering the unique challenges posed by this global health crisis. Data scarcity is a fundamental issue; COVID-19 is a novel disease, and collecting a large and diverse dataset for COVID-19-specific deep learning models is challenging, given the urgency of the situation. Transfer learning mitigates this limitation by allowing the application of pre-trained models' knowledge, bridging the gap between data availability and model requirements.

Furthermore, the rapid deployment of diagnostic tools during a pandemic is essential. Developing a deep learning model from scratch is a time-consuming process that can delay the response to the virus's spread. Transfer learning accelerates the model development process, enabling healthcare professionals to quickly access effective COVID-19 diagnostic tools. This factor is particularly critical during a global pandemic where timely diagnosis is vital for patient care and disease management. Ultimately, transfer learning not only enhances accuracy in COVID-19 detection by leveraging pre-learned image features but also plays a crucial role in addressing the global impact of the pandemic, potentially saving lives through swift and precise identification of affected individuals.

Transfer learning relies on the straightforward idea of applying the expertise of a model trained on a large image dataset to another dataset and hence attracts researcher interest for image classification with outstanding performance. Convolutional Neural Network, generally known as CNN, facilitates the use of transfer learning and excels the performance for image classifications. In our model, we feed the preprocess image data to different types of pre-train CNN also known as transfer learning model including Xception, InceptionResNetV2, ResNet50, ResNet50V2, EfficientNetB0 and EfficientNetB4. What follows we describe the architecture of each model for the experiments.

- Xception: Xception, the extreme form of Inception, is an architecture built on depth-wise separable convolutional layers. With this enhanced depth-wise separable convolution, it performs significantly better than Inceptionv3 Chollet (2017). The Xception architecture, a modification of the Inception architecture, takes the place of the normal Inception modules. The architecture is straightforward and flexible. The architecture's 36 convolution layers serve as the foundation to extract functions from the network. Except for the first and last modules, these 36 layers are divided into 14 modules, each of which is connected to the others by linear threads. The depth-wise detachable convolution layers will combine to form a linear stack with lingering connections Tsang (2018).

- InceptionResNetV2: An incorporation of residual connections into the deep inception network is known as InceptionResNetV2 Szegedy et al. (2017). The model outperformed batch normalization-Inception, Inception-v3, Inception-Resnet-v1, and Inception-v4 in top-1 and top-5 error rates Ramanna et al. (2021).
- Residual Network (ResNet): ResNet is a potent backbone model commonly employed in numerous computer vision tasks. By using the skip connection, ResNet can tackle the vanishing gradient problem, in which the gradient's value decreases noticeably He et al. (2016a).

ResNet50 is a pre-trained convolutional neural network and a variation of the ResNet model with 50 layers total, 48 of which are convolutional neural networks and the remaining two being average and max pool layers Reddy and Juliet (2019).

A customized variant of ResNet50, known as ResNet50V2 He et al. (2016b), outperforms ResNet50 as well as ResNet101 on the ImageNet dataset. The propagating concept of the links between blocks was changed in ResNet50V2 to reflect this change Rahimzadeh and Attar (2020).

- EfficientNet: EfficientNet is an architectural and scaling technique for convolutional neural networks that uses a compound coefficient to scale all depth, breadth, and resolution dimensions evenly Tan and Le (2019).

A baseline architecture that is optimized and a scaling strategy that is effective are two pillars upon which the EfficientNet family is built. The foundational network, EfficientNet B0, is composed of 2D Depthwise convolution blocks, which have been proven to be incredibly efficient in terms of both processing time and cost. Using more than a million photos from the ImageNet collection, the convolutional neural network EfficientNet-b0 was trained Tan et al. (2019).

The typical approach to improving image classification accuracy is to start with an existing network, increase its depth by increasing the number of layers that data passes through, increase its width by increasing the number of filters in each layer, and feed the network images with higher resolutions that contain more and finer details. These three components are scaled up together by EfficientNets to boost accuracy in a ratio that has been designed to prevent any one of them from ever becoming a bottleneck. By scaling up EfficientNet B0 in this manner, a network with nearly four times as much processing power, EfficientNet B4, is produced Tan and Le (2019).

3.5. Fine Tuning Process

In our research, the fine-tuning process is a critical step in adapting pre-trained neural network models to excel in the specific task of COVID-19 detection using radiological imagery. This section provides a comprehensive insight into our approach, including an extensive discussion of the hyperparameters employed and the rationale behind the selection of each value.

3.5.1. Overview Fine-Tuning Process

In our studies, the fine-tuning process began with resizing the input images to dimensions of 256x256x3, thereby preprocessing the images to ensure uniformity. Subsequently, for each transfer learning model, we executed the following steps:

- **Layer Modification:** The last layers beyond the last activation layer were removed. In their place, we introduced global average pooling, batch normalization, dense layers, dropout layers with a dropout rate of 0.2, ReLU activation layers, and concluded with a softmax fully connected layer for binary classification.
- **Fine-Tuning Strategy:** To facilitate the adaptation of the pre-trained models to our specific task, we implemented fine-tuning. This involved unfreezing the entire model and retraining it using a notably low learning rate of 0.001. The rationale behind this approach is to iteratively adjust the pre-trained features to align with the characteristics of our new image data.

Figure 5 shows the fine-tuned process on an existing transfer learning model. By executing the fine-tuning process, we aimed to harness the power of transfer learning while tailoring the models to our COVID-19 detection task. The combination of leveraging pre-trained features and adjusting them to our dataset has the potential to yield significant enhancements in detection performance.

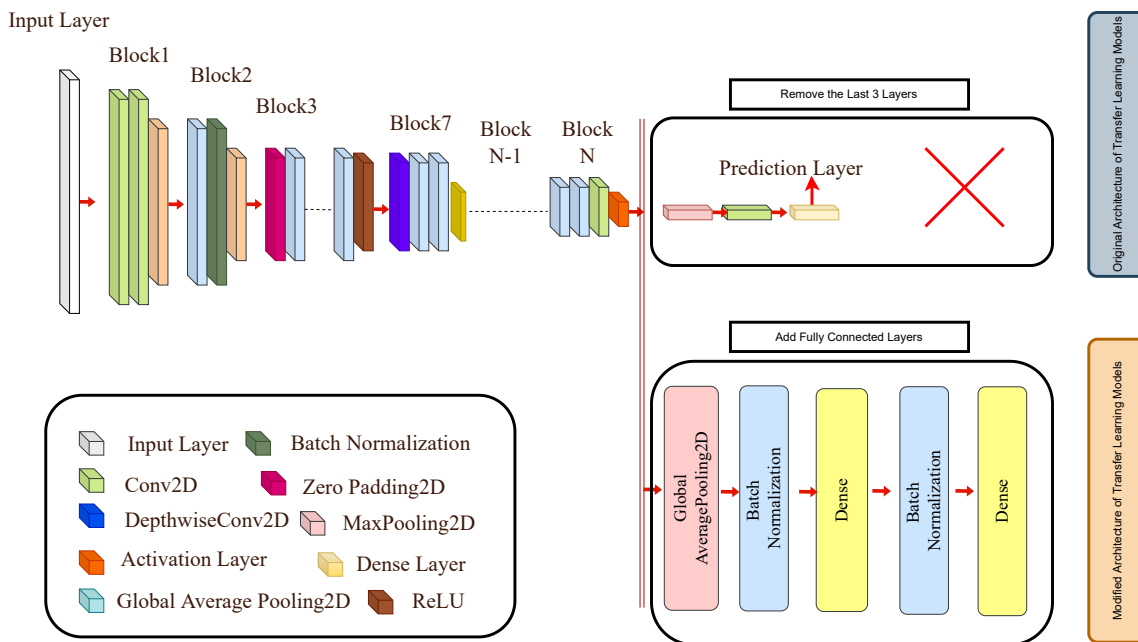


Figure 5: The proposed modification of transfer learning architecture

3.5.2. Hyperparameter Tuning

1. **Random Seed (seed=1000):** The use of a fixed random seed is pivotal in ensuring the reproducibility of our experiments. By setting the seed to a specific value (seed=1000), we guarantee that each run of our model will produce consistent results. This reproducibility is essential in scientific research and facilitates the comparison of our findings with other studies.
2. **Learning Rate (lr=0.0001):** The learning rate is a hyperparameter that governs the magnitude of updates to the model's parameters during training. We selected a learning rate of 0.0001 based on a careful balance between convergence speed and stability. This rate allows for gradual parameter adjustments, preventing overshooting during optimization. It is well-suited for our COVID-19 detection task, ensuring steady progress in training while avoiding erratic behavior.

3. **Activation Function (ReLU):** We opted for Rectified Linear Unit (ReLU) as the activation function in our densely connected layers. ReLU has gained popularity in deep learning due to its effectiveness in mitigating the vanishing gradient problem and accelerating convergence. It introduces non-linearity into the model, allowing it to capture complex features in the data. ReLU is a suitable choice for our task as it helps the network learn and represent intricate patterns in radiological images, leading to improved diagnostic accuracy.
4. **Model Architecture and Architectural Elements:** We selected the model architecture from a range of options, including Xception, InceptionResNetV2, ResNet50, ResNet50V2, EfficientNetB0, and EfficientNetB4. The choice of architecture was made based on their proven performance in various computer vision tasks and their ability to handle different complexities of radiological images. These architectures have been fine-tuned to optimize COVID-19 detection.
5. **GlobalMaxPooling2D and BatchNormalization:** To enhance the model's feature extraction capabilities and improve training stability, we introduced GlobalMaxPooling2D layers for global feature extraction and Batch-Normalization layers for normalizing the input data. These architectural elements contribute to effective information abstraction and model convergence.
6. **Dropout Layer (dropout rate of 0.001):** A dropout layer with a dropout rate of 0.001 was incorporated to prevent overfitting, which can occur when the model becomes too specialized to the training data. By randomly dropping out a small fraction of neurons during training, the model generalizes better to new data, enhancing its ability to make accurate predictions.
7. **Dense Layer:** The Dense layer plays a vital role in capturing intricate patterns in radiological images. It facilitates the transformation of extracted features into meaningful predictions, making it a critical component for accurate diagnosis. This layer contributes to the model's capacity to classify COVID-19 cases based on the learned patterns in the data.
8. **Softmax Activation Output Layer:** We employed a softmax-activated output layer for classification. This layer assigns probabilities to the different classes, allowing us to classify radiological images into relevant categories effectively.

The fine-tuning process concludes with the compilation of the model using an Adam optimizer, enabling all layers within the model to be trainable. The model's performance is evaluated using the Sparse Categorical Cross-Entropy loss function and the accuracy metric.

4. Experimental Setup and Evaluation Metrics

4.1. Experimental Setup

The experiments were conducted on a computer system with the following specifications: an Intel Core i7 processor, 16GB RAM, a 4 GB graphics card, and a 64-bit Windows operating system running at a clock speed of 1.80 GHz. The experiments were implemented using the Python programming language and essential libraries such as pandas, numpy, matplotlib, keras, and tensorflow were utilized. During the experimental process, the image dataset was divided into three distinct groups: training, testing, and validation for 80%, 10% and 10%, respectively.

The training and validation sets were employed for model training. Subsequently, the models' performance was evaluated using the dedicated testing dataset. Table 1 shows the data distribution used in our experiment.

Dataset	Training	Validation	Testing
COVID-19 X-Ray	1600	192	208
Chest X-Ray	3456	416	480

Table 1: Dataset Distribution in experiment

4.2. Data Splitting

In our research, we adopted a standard data split for training, validation, and testing, with the following percentages:

- Training Set: 80% of the image dataset was allocated for training the deep learning model.
- Validation Set: An additional 10% of the dataset was reserved for validation purposes. This set was used to fine-tune the model, optimize hyperparameters, and monitor training progress.
- Testing Set: The remaining 10% of the dataset served as the dedicated testing dataset, used exclusively for evaluating the final performance of the models. This dataset allowed us to assess the model's generalization capabilities and its effectiveness in making predictions on unseen data.

By dividing the dataset into these three subsets with the specified ratios, we aimed to strike a balance between training the model, tuning its parameters, and rigorously testing its performance on previously unseen data.

4.3. Handling Overfitting

In our research, we recognized the critical importance of mitigating overfitting, which occurs when a machine learning model performs exceptionally well on the training data but struggles to generalize to new, unseen data. Overfitting can compromise the practical utility of the model, especially in clinical applications like COVID-19 detection.

4.3.1. Methods to Address Overfitting

- Data Augmentation: To increase the diversity of our training dataset and reduce the risk of overfitting, we employed data augmentation techniques. Data augmentation involves creating new training samples by applying random transformations to the existing data, such as rotation, scaling, and flipping. This process enhances the model's ability to generalize by exposing it to a wider range of image variations.
- Dropout Layers: We incorporated dropout layers in our model architecture to prevent overfitting. Dropout layers randomly deactivate a fraction of neurons during training, essentially creating an ensemble of different network architectures for each batch of data. This regularization technique discourages the network from relying too heavily on any particular feature, contributing to better generalization.

- **Appropriate Model Complexity:** We carefully selected model architectures and hyperparameters to strike a balance between model complexity and the size of our dataset. Complex models are more prone to overfitting, so we aimed to keep our models appropriately sized for the task at hand.
- **Cross-Validation:** We performed cross-validation to evaluate the model's performance across multiple folds of the data. This technique helps us assess the model's consistency in making predictions and guards against overfitting to a specific subset of the data.

By implementing these methods, we strived to ensure that our models maintain a strong ability to generalize to new, unseen data, enhancing their reliability for COVID-19 detection.

4.4. Performance Metrics

The covid-19 detection model performance assessment relies heavily on utilizing the confusion matrix. This invaluable tool offers a comprehensive summary of predicted and actual class labels, facilitating the evaluation of true positives (TP), true negatives (TN), false positives (FP), and false negatives (FN). Displayed in Table 2, this visual representation yields insights into a model's accuracy, precision, recall, and F1-score, which are pivotal for measuring its efficacy across different classes. By illustrating classification outcomes, the confusion matrix guides model refinement and decision-making in COVID-19 detection.

Predicted Results	Actual Positive	Actual Negative
Yes	TP	FP
No	FN	TN

Table 2: Confusion Matrix.

Several crucial performance metrics are employed for evaluating the effectiveness of deep learning models, each serving a distinct purpose:

Accuracy: This fundamental metric represents the proportion of correctly predicted outcomes to the total number of observations. Higher accuracy values indicate superior model performance and can be calculated using the equation:

$$Accuracy = \frac{TP + TN}{TP + FP + FN + TN} \quad (1)$$

Precision: Precision gauges the quality of a deep learning algorithm by indicating the proportion of accurately predicted positive observations to all predicted positive instances. It is defined as:

$$Precision = \frac{TP}{TP + FP} \quad (2)$$

Recall: Also known as sensitivity or true positive rate, recall measures the proportion of correctly predicted positive outcomes to all actual positive instances:

$$Recall = \frac{TP}{TP + FN} \quad (3)$$

F1-Score: The F1-score offers a balanced assessment of a model's precision and recall, calculated as the harmonic mean of these two metrics:

$$F1_{score} = 2 \cdot \frac{(Precision \cdot Recall)}{(Precision + Recall)} \quad (4)$$

Additional metrics used for performance evaluation include:

Mean Absolute Error (MAE):

$$MAE = \frac{\sum_{i=1}^n |predict(i) - actual(i)|}{n} \quad (5)$$

Mean Squared Error (MSE):

$$MSE = \frac{\sum_{i=1}^n (predict(i) - actual(i))^2}{n} \quad (6)$$

Root Mean Squared Error (RMSE):

$$RMSE = \sqrt{\frac{\sum_{i=1}^n (predict(i) - actual(i))^2}{n}} \quad (7)$$

Mean Absolute Error (MAE) is crucial in our study as it quantifies the average magnitude of errors between the predicted and actual values, helping us understand the typical discrepancy in COVID-19 detection. Mean Squared Error (MSE) is included to reveal average squared differences, particularly relevant for penalizing larger errors, aiding in identifying outliers with significant clinical implications. Root Mean Squared Error (RMSE), used alongside MSE, provides error values in the same unit as the predicted and actual values, offering a more interpretable perspective on prediction error magnitude and facilitating a clearer understanding of model performance.

In our study, these metrics were chosen to provide a holistic view of the model's performance by assessing both the average and the dispersion of prediction errors. MAE, MSE, and RMSE collectively contribute to a comprehensive evaluation of our models in the context of COVID-19 detection, ensuring a balanced assessment of their accuracy and the practical implications of their predictions.

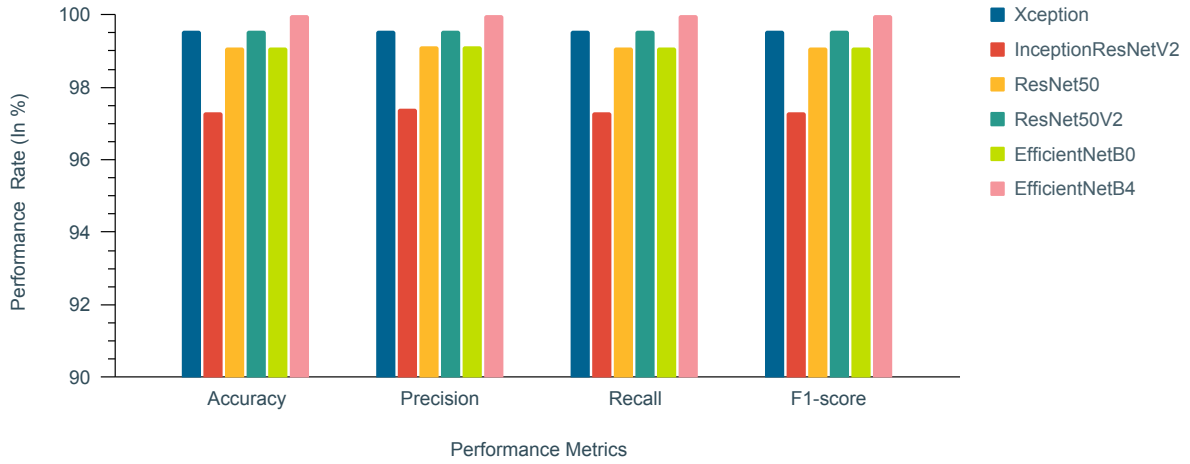
5. Result Analysis

In our experiment, we used two datasets such as COVID-19 X-Ray Image and Chest X-Ray Image to prove our model's efficiency in terms of performance evaluations to correctly detection of COVID-19 disease.

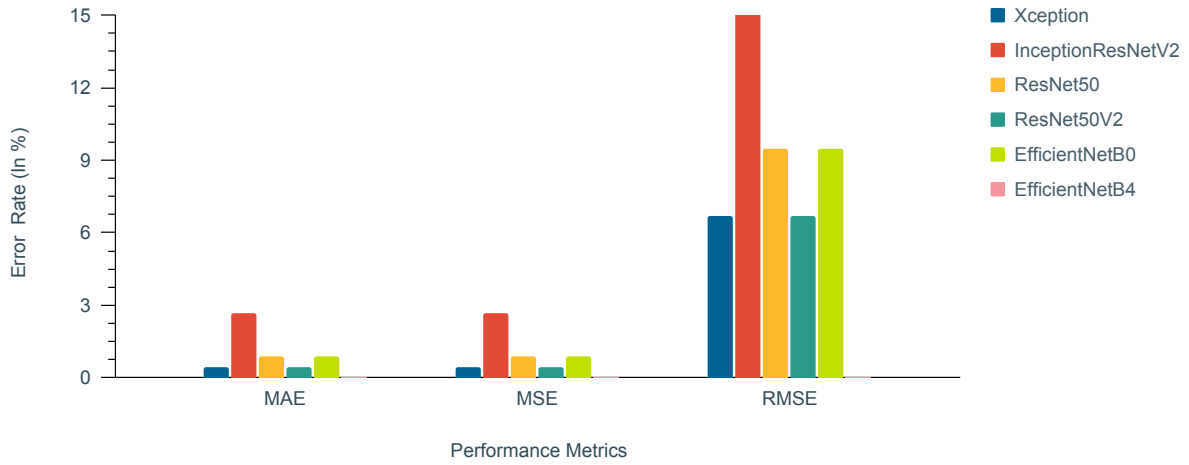
5.1. Result Analysis of COVID-19 X-Ray Dataset

The evaluation of fine-tuned deep learning models for COVID-19 detection reveals insightful findings as summarized in Table 3 and Figure 6 illustrates the results in pictorial form. This comprehensive analysis delves into various performance metrics that illuminate the effectiveness of each model in accurately identifying COVID-19 cases from medical images.

The performance analysis, as presented in Table 3, revolves around the crucial accuracy metric, which measures the models' overall effectiveness in correctly classifying COVID-19 cases. Among the diverse set of models evaluated, EfficientNetB4 stands out as the exemplar with a perfect accuracy rate of 100%. This remarkable accuracy underscores its exceptional proficiency in accurately distinguishing between COVID-19 positive and negative cases. Other models also demonstrate commendable accuracy rates: Xception achieves a high accuracy of 99.55%, ResNet50 and ResNet50V2 achieve an accuracy of 99.11% and 99.55%, respectively, while EfficientNetB0 attains



(a) Performance



(b) Error

Figure 6: The performance Results of Covid19 Xray dataset.

DL Model	Accuracy	Precision	Recall	F1-score	MAE	MSE	RMSE
Xception	99.55	99.56	99.55	99.55	0.45	0.45	6.68
InceptionResNetV2	97.32	97.4	97.31	97.32	2.68	2.68	16.37
ResNet50	99.11	99.13	99.1	99.11	0.89	0.89	9.45
ResNet50V2	99.55	99.56	99.55	99.55	0.45	0.45	6.68
EfficientNetB0	99.11	99.13	99.1	99.11	0.89	0.89	9.45
EfficientNetB4	100	100	100	100	0	0	0

Table 3: Performance analysis of DL models

an accuracy rate of 99.11%. InceptionResNetV2, with an accuracy of 97.32%, maintains a strong performance level. These accuracy values collectively underscore the models' competence in making accurate predictions and highlight their potential for effective COVID-19 detection.

When considering precision, which measures the models' ability to predict positive cases among the predicted positives accurately, we observe a range from 97.31% (InceptionResNetV2) to a perfect 100% (EfficientNetB4). Similarly, recall, which indicates the models' capacity to identify actual positives among all actual positive cases, spans from 97.31% (InceptionResNetV2) to a flawless 100% (EfficientNetB4). The F1-score, a balance between precision and recall, mirrors this pattern, ranging from 97.32% (InceptionResNetV2) to 100% (EfficientNetB4), reflecting the models' effectiveness in both true positive prediction and positive class identification.

Turning to projection error metrics, MAE, capturing the average absolute difference between predicted and actual values, ranges from 0 (EfficientNetB4) to 2.68 (InceptionResNetV2), reflecting the precision of the models' numerical predictions. MSE, calculating the average of squared prediction errors, spans from 0 (EfficientNetB4) to 2.68 (InceptionResNetV2), emphasizing the models' overall predictive accuracy. RMSE, the square root of MSE, ranges from 0 (EfficientNetB4) to 16.37 (InceptionResNetV2), encapsulating both magnitude and direction of prediction errors and providing an overall measure of prediction accuracy.

The confusion matrix, a pivotal tool in evaluating the performance of covid-19 detection models, provides an insightful snapshot of the models' predictive outcomes in terms of TP, TN, FP, and FN instances. The confusion matrix is illustrated in Figure 7. For the Xception model, the matrix illustrates 113 true positive predictions and 110 true negative predictions, with a single false positive and a single false negative prediction. In the case of InceptionResNetV2, there are 112 true positive predictions and 106 true negative predictions, accompanied by one false positive and five false negative predictions. Similarly, ResNet50 attains 113 true positive predictions and 109 true negative predictions, with two false positives and no false negative predictions. The ResNet50V2 model mirrors the pattern of 113 true positive and 110 true negative predictions, with one false positive and no false negative predictions. EfficientNetB0's matrix also reflects 113 true positive predictions and 109 true negative predictions, accompanied by two false positives and no false negative predictions. Lastly, EfficientNetB4 stands out with a perfect matrix of 113 true positive predictions and 111 true negative predictions, highlighting its exceptional accuracy in both true positives and true negatives, with no false positive or false negative predictions. This comprehensive set of confusion matrices provides valuable insights into the predictive strengths and limitations of each model across

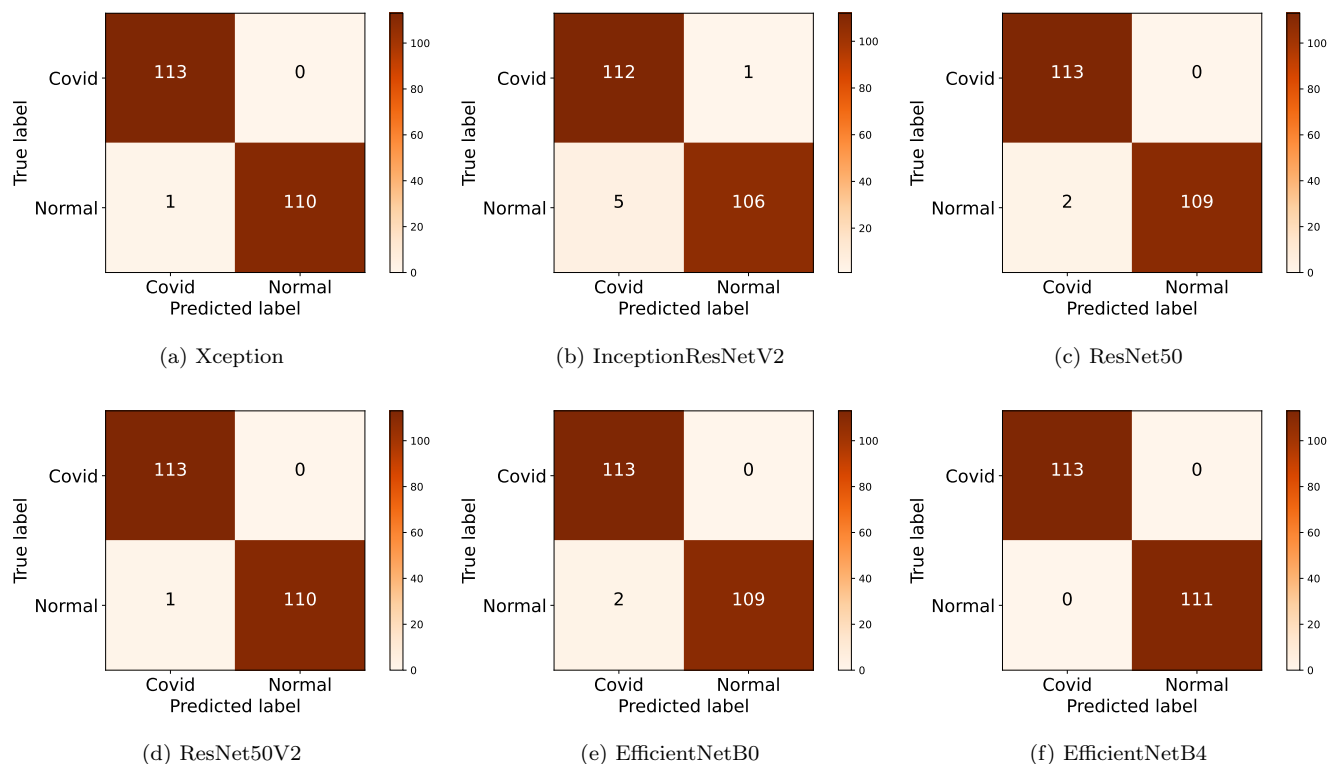


Figure 7: Confusion Matrix of DL models

different classification outcomes.

Figure 8 depicts the training and validation accuracy during the experiments. The Y-axis represents the learning accuracy and X-axis represents the experiences for any algorithms. As we can see, with the increasing order of the epoch over time increases the training and validation accuracy. For any case, the training accuracy after 5 epochs and remains constant and validation accuracy reaches a steady state after 15 epochs. As a result, the curves demonstrate a satisfactory level of fitting for every model under consideration, both during the training phase and the validation test.

The time-varying loss curve for the training and validation sets is shown in Figure 9. The loss of the models decreases and stays closer to the training loss, demonstrating well-fitting characteristics, as shown by the graphs. While the validation loss was initially higher for ResNet50 and EfficientNetB4 up to epoch 15, it eventually leveled off and moved closer to the training loss, which displays the best-fit curves.

Among the evaluated models, EfficientNetB4 stands out as the indisputable best performer. Achieving perfect scores across all performance metrics, including accuracy, precision, recall, and F1-score, showcases unparalleled accuracy in detecting COVID-19 cases from medical images. Notably, EfficientNetB4 also demonstrates zero prediction error, making it an exceptional choice for real-world application. This model's outstanding performance signals its potential to revolutionize medical diagnostics and contribute significantly to global efforts in managing and mitigating the ongoing pandemic.

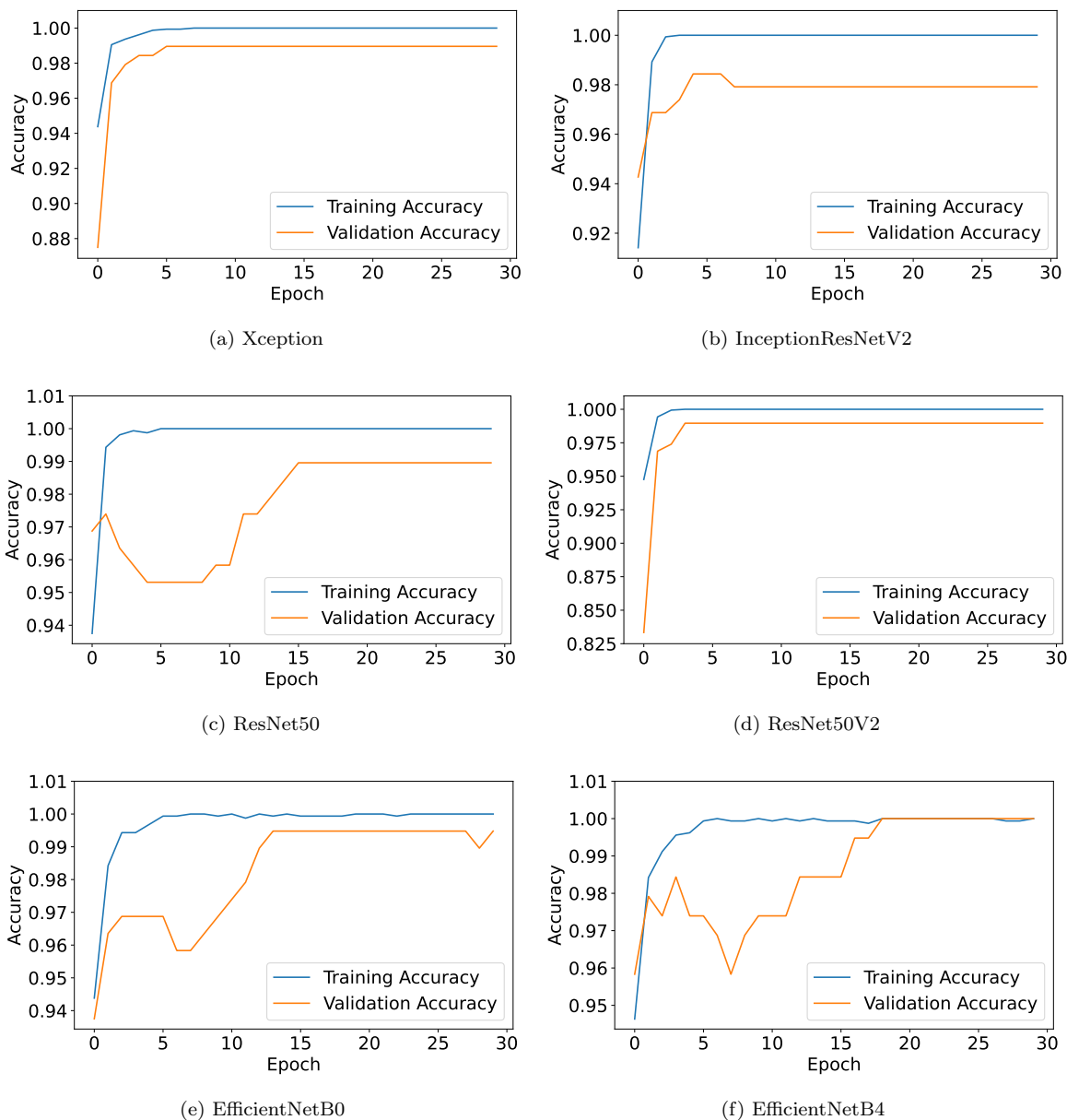


Figure 8: Accuracy Graph of DL models

5.1.1. Discussion

The discussion section delves into the performance analysis of different deep learning models fine-tuned for COVID-19 detection using the COVID19 X-Ray dataset illustrated in Table 4. The models evaluated include Xception, InceptionResNetV2, ResNet50, ResNet50V2, EfficientNetB0, and EfficientNetB4, each of which underwent fine-tuning to enhance their suitability for COVID-19 detection. The dataset comprised 2000 COVID19 X-Ray images, and the primary performance metric, accuracy in percentage, was used to assess the models' effectiveness.

The performance results reveal noteworthy achievements across the models. Among the evaluated models, EfficientNetB4 stood out, achieving a remarkable accuracy score of 100%, thereby exhibiting the potential for highly accurate COVID-19 detection. Following closely, Xception and ResNet50V2 also demonstrated commendable

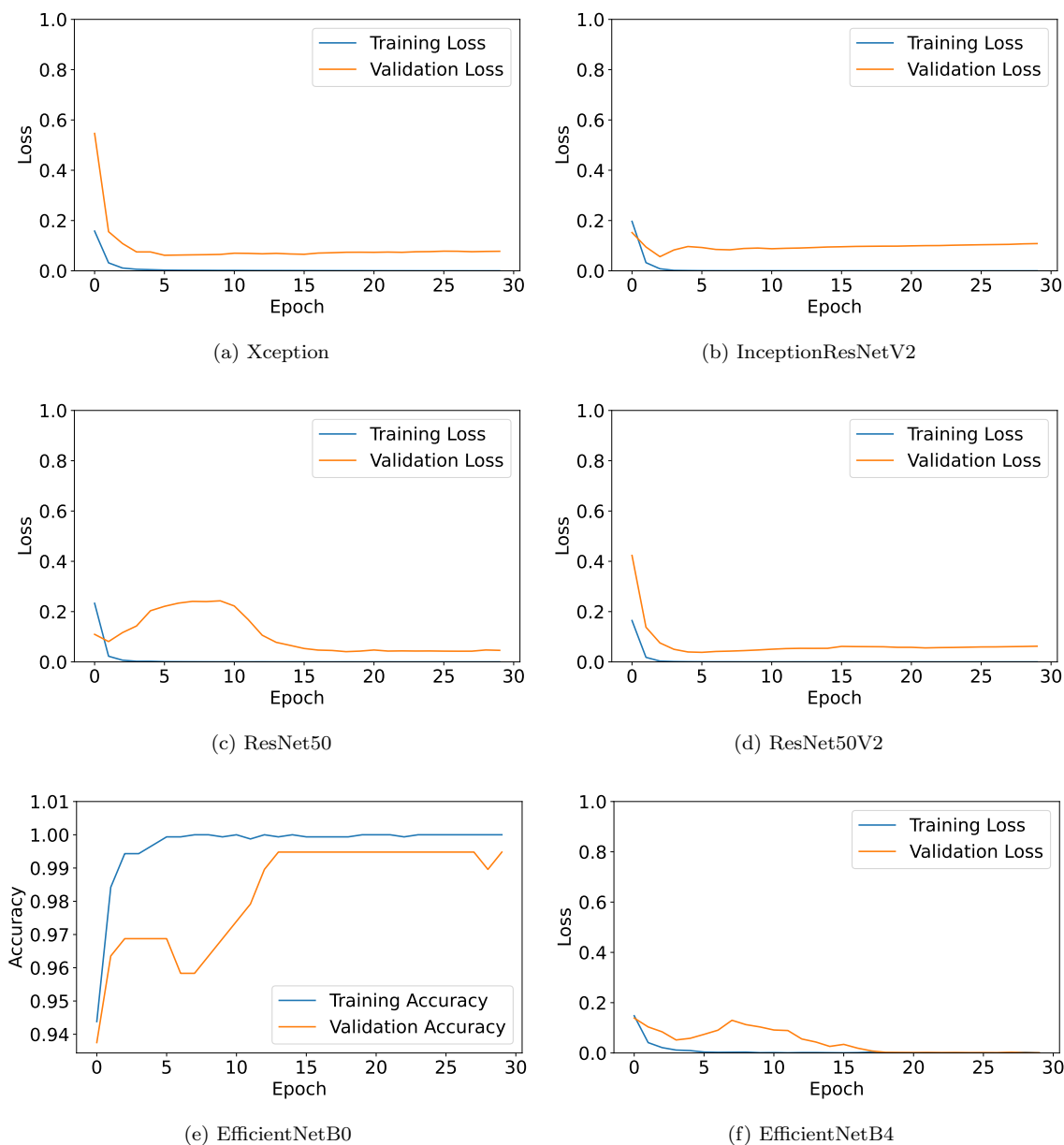


Figure 9: Loss Graph of DL models

performance, both achieving an accuracy of 99.55%, underlining their effectiveness in distinguishing COVID-19 cases from X-ray images. InceptionResNetV2 and ResNet50 achieved accuracy scores of 97.32% and 99.11%, respectively. These scores, while slightly lower than the top-performing models, still demonstrate a high degree of accuracy in COVID-19 detection using X-ray images. EfficientNetB0, with an accuracy of 99.11%, further reinforces the robustness of efficient neural architectures in this context.

The outcomes affirm that fine-tuning deep learning models significantly contributes to their diagnostic capabilities for COVID-19. The high accuracy achieved by various models indicates their potential to serve as reliable tools for medical practitioners in identifying COVID-19 cases through X-ray images. The variations in accuracy scores between models emphasize the importance of selecting an appropriate architecture for a specific diagnostic task.

It is important to acknowledge that the presented accuracy scores represent real-world scenarios of collected data. Nevertheless, the results provide valuable insight into the capabilities of different DL models for COVID-19 detection from X-ray images. Among all, EfficientnetB4 provides comprehensive better results than others, which can help in aiding the development of accurate and reliable diagnostic tools for effective pandemic management.

Model	Method	Dataset	No. of Images	Performance (Accuracy in %)
Xception	Xception + Fine-Tuning	COVID19 X-Ray	2000	99.55
InceptionResNetV2	InceptionResNetV2 + Fine-Tuning	COVID19 X-Ray	2000	97.32
ResNet50	ResNet50 + Fine-Tuning	COVID19 X-Ray	2000	99.11
ResNet50V2	ResNet50V2 + Fine-Tuning	COVID19 X-Ray	2000	99.55
EfficientNetB0	EfficientNetB0 + Fine-Tuning	COVID19 X-Ray	2000	99.11
Proposed (EfficientNetB4)	EfficientNetB4 + Fine-Tuning	COVID19 X-Ray	2000	100

Table 4: Comparison analysis of proposed Fine-Tuned DL model with others on COVID-19 Data

The exploration of solutions to address the aforementioned concerns involves proposing methodologies for the following inquiries: Firstly, how to formulate an optimal automated COVID detection model that not only enhances accuracy but also effectively tackles the limitations evident in current solutions. Secondly, how to seamlessly integrate this novel detection model with COVID-19 datasets, ensuring harmonious compatibility to capitalize on its potential for achieving precise predictions. Lastly, how to fine-tune and optimize existing models to attain significantly heightened levels of accuracy, thereby reinforcing the reliability and efficacy of COVID-19 detection mechanisms.

5.1.2. Complexity Analysis

The complexity analysis of the prediction table revolves around the interplay between prediction speed and model accuracy in various DL models. In this context, complexity refers to the balance between computational efficiency and predictive capability. Table 5 presents prediction speeds, measured in seconds per prediction, as indicators of computational efficiency. Notably, ResNet50V2 emerges as the quickest, requiring just 16 seconds. Xception, ResNet50, and EfficientNetB0 share a marginally slower speed at 18 seconds. InceptionResNetV2 and the Proposed (EfficientNetB4) model demand 30 seconds for a prediction, marking them as the slowest. The note about the proposed EfficientNetB4 model adds an accuracy dimension to the analysis. Although it matches InceptionResNetV2 in prediction speed, it promises the highest accuracy. This illustrates the inherent trade-off: higher accuracy often necessitates more complex models, prolonging prediction times. In practice, choosing a model entails considering trade-offs. For tasks valuing precision over real-time response, EfficientNetB4 could excel. Conversely, time-sensitive applications might favor quicker models like ResNet50V2, compromising some accuracy. The analysis underscores the delicate balance between prediction speed, accuracy, and model complexity. This understanding empowers decision-makers to select models aligning with specific needs, optimizing the intricate relationship between computational efficiency and predictive performance.

DL Model	Prediction Speed (In sec)
Xception	18
InceptionResNetV2	30
ResNet50	18
ResNet50V2	16
EfficientNetB0	18
Proposed (EfficientNetB4)	30

Table 5: Prediction Speeds of Different DL Models

5.2. Result Analysis of Chest X-Ray Dataset

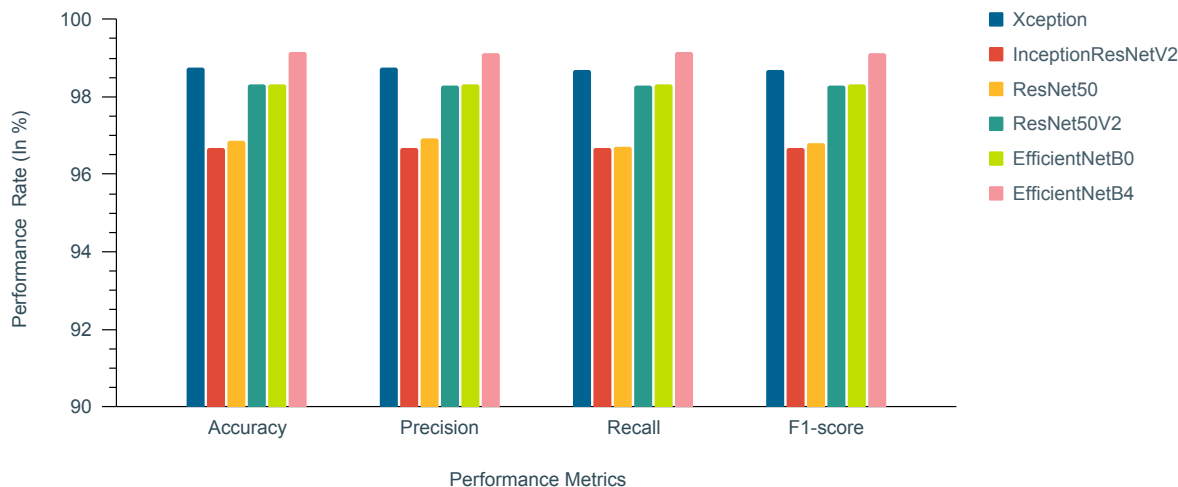
The evaluation of fine-tuned deep learning models for Lung Disease detection reveals insightful findings as summarized in Table 6 and Figure 10 illustrates the results in pictorial form. This comprehensive analysis delves into various performance metrics that illuminate the effectiveness of each model in accurately identifying lung disease from medical images.

DL Model	Accuracy	Precision	Recall	F1-score	MAE	MSE	RMSE
Xception	98.75	98.75	98.68	98.7	1.25	1.25	11.18
InceptionResNetV2	96.67	96.68	96.67	96.67	4.17	5.83	24.15
ResNet50	96.88	96.94	96.71	96.79	3.54	4.38	20.92
ResNet50V2	98.33	98.28	98.28	98.28	2.08	2.92	17.08
EfficientNetB0	98.33	98.31	98.31	98.31	2.29	3.54	18.82
EfficientNetB4	99.17	99.13	99.16	99.14	1.25	2.08	14.43

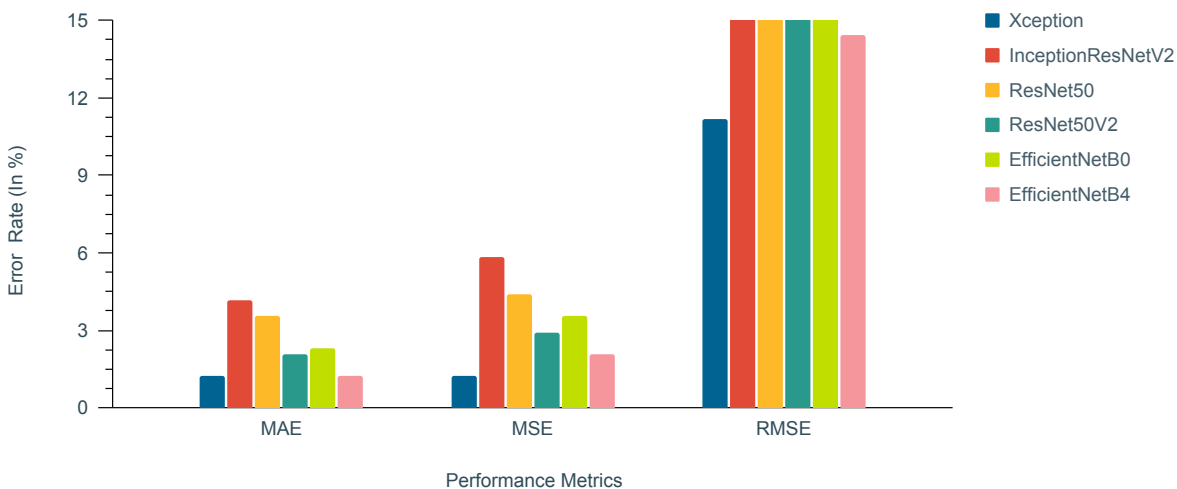
Table 6: Performance analysis of DL models

The performance analysis, as presented in Table 6, revolves around the crucial accuracy metric, which measures the models' overall effectiveness in correctly classifying Lung disease cases. Among the diverse set of models evaluated, EfficientNetB4 stands out as the exemplar with a perfect accuracy rate of 99.17%. This remarkable accuracy underscores its exceptional proficiency in accurately distinguishing among COVID-19, Lung opacity, Normal and Viral Pneumonia cases. Other models also demonstrate commendable accuracy rates: Xception achieves a high accuracy of 98.75%, ResNet50 and InceptionResNetV2 achieve an accuracy of 96.88% and 96.67%, respectively, while EfficientNetB0 attains an accuracy rate of 98.33%. ResNet50V2, with an accuracy of 98.33%, maintains a strong performance level. These accuracy values collectively underscore the models' competence in making accurate predictions and highlight their potential for effective lung disease detection.

When considering precision, which measures the model's ability to predict positive cases among the predicted positives accurately, we observe a range from 96.68% (InceptionResNetV2) to a perfect 99.13% (EfficientNetB4). Similarly, recall, which indicates the models' capacity to identify actual positives among all actual positive cases, spans from 96.67% (InceptionResNetV2) to a flawless 99.16% (EfficientNetB4). The F1-score, a balance between precision and recall, mirrors this pattern, ranging from 96.67% (InceptionResNetV2) to 99.14% (EfficientNetB4),



(a) Performance



(b) Error

Figure 10: The performance Results of Chest X-Ray dataset.

reflecting the models' effectiveness in both true positive prediction and positive class identification.

Turning to projection error metrics, MAE, capturing the average absolute difference between predicted and actual values, ranges from 1.25 (EfficientNetB4) to 4.17 (InceptionResNetV2), reflecting the precision of the models' numerical predictions. MSE, calculating the average of squared prediction errors, spans from 2.08 (EfficientNetB4) to 5.83 (InceptionResNetV2), emphasizing the models' overall predictive accuracy. RMSE, the square root of MSE, ranges from 11.18 (Xception) to 24.15 (InceptionResNetV2), encapsulating both magnitude and direction of prediction errors and providing an overall measure of prediction accuracy.

The confusion matrix, a pivotal tool in evaluating the performance of Lung disease detection models, provides an insightful snapshot of the models' predictive outcomes in terms of TP, TN, FP, and FN instances. The confusion matrix is illustrated in Figure 11.

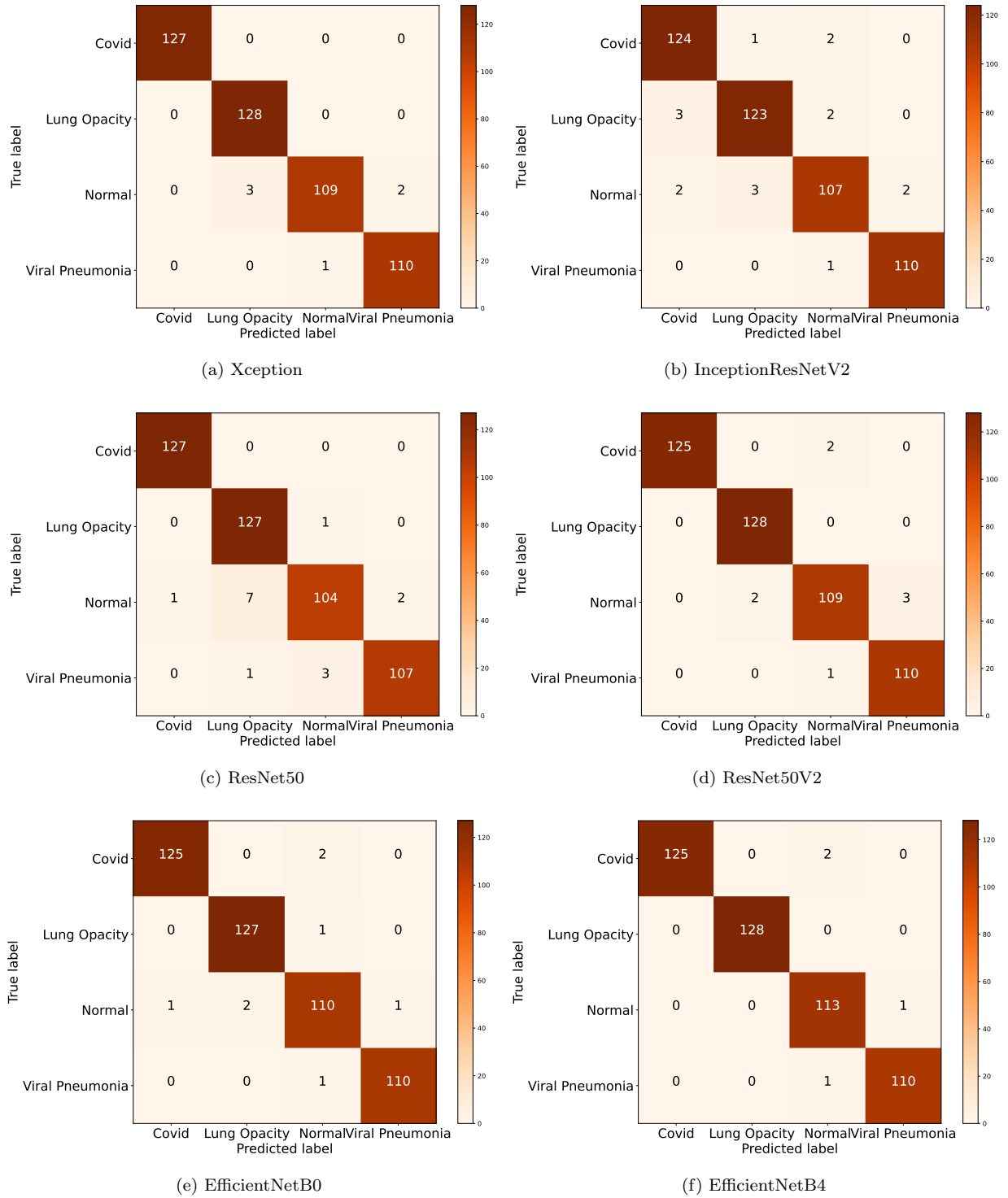


Figure 11: Confusion Matrix of DL models

For the Xception model, the matrix of Figure 11(a) illustrates for the COVID class 127 true positive predictions and 353 true negative predictions, with 0 false positive and 0 false negative predictions; for Lung-Opacity class 128 true positive predictions and 349 true negative predictions, with 3 false positive and 0 false negative predictions; for Normal class 109 true positive predictions and 365 true negative predictions, with 1 false positive and 5 false negative predictions; for Viral Pneumonia class 110 true positive predictions and 367 true negative predictions, with 2 false positive and 1 false negative predictions;

For the InceptionResNetV2 model, the confusion matrix of Figure 11(b) shows the following results: COVID class: 124 true positive predictions and 348 true negative predictions, with 5 false positives and 3 false negative predictions. Lung-Opacity class: 123 true positive predictions and 348 true negative predictions, with 4 false positives and 5 false negative predictions. Normal class: 107 true positive predictions and 361 true negative predictions, with 5 false positives and 7 false negative predictions. Viral Pneumonia class: 110 true positive predictions and 367 true negative predictions, with 2 false positives and 1 false negative prediction.

For the ResNet50 model, the confusion matrix of Figure 11(c) reveals the following outcomes: COVID class: 127 true positive predictions and 352 true negative predictions, with 1 false positive and 0 false negative predictions. Lung-Opacity class: 127 true positive predictions and 344 true negative predictions, with 8 false positives and 1 false negative prediction. Normal class: 104 true positive predictions and 362 true negative predictions, with 4 false positives and 10 false negative predictions. Viral Pneumonia class: 107 true positive predictions and 367 true negative predictions, with 2 false positives and 4 false negative predictions.

The confusion matrix of Figure 11(d) for the ResNet50V2 model illustrates the following statistics: COVID class: 125 true positive predictions and 353 true negative predictions, with 0 false positives and 2 false negative predictions. Lung-Opacity class: 128 true positive predictions and 350 true negative predictions, with 2 false positives and 0 false negative predictions. Normal class: 109 true positive predictions and 363 true negative predictions, with 3 false positives and 5 false negative predictions. Viral Pneumonia class: 110 true positive predictions and 366 true negative predictions, with 3 false positives and 1 false negative prediction.

The confusion matrix of Figure 11(e) for the EfficientNetB0 model displays the following results: COVID class: 125 true positive predictions and 352 true negative predictions, with 1 false positive and 2 false negative predictions. Lung-Opacity class: 127 true positive predictions and 350 true negative predictions, with 2 false positives and 1 false negative prediction. Normal class: 110 true positive predictions and 362 true negative predictions, with 4 false positives and 4 false negative predictions. Viral Pneumonia class: 110 true positive predictions and 368 true negative predictions, with 1 false positive and 1 false negative prediction.

For the EfficientNetB4 model, the confusion matrix of Figure 11(f) reveals the following outcomes: COVID class: 125 true positive predictions and 353 true negative predictions, with 0 false positives and 2 false negative predictions. Lung-Opacity class: 128 true positive predictions and 352 true negative predictions, with 0 false positives and 0 false negative predictions. Normal class: 113 true positive predictions and 363 true negative predictions, with 3 false positives and 1 false negative prediction. Viral Pneumonia class: 110 true positive predictions and 368 true negative predictions, with 1 false positive and 1 false negative prediction. These detailed descriptions of the confusion matrices provide valuable insights into the predictive performance of each deep learning model across various classes, highlighting their ability to correctly classify true positives and true negatives while also indicating

areas where they may make false positive or false negative predictions.

This comprehensive set of confusion matrices provides valuable insights into the predictive strengths and limitations of each model across different classification outcomes.

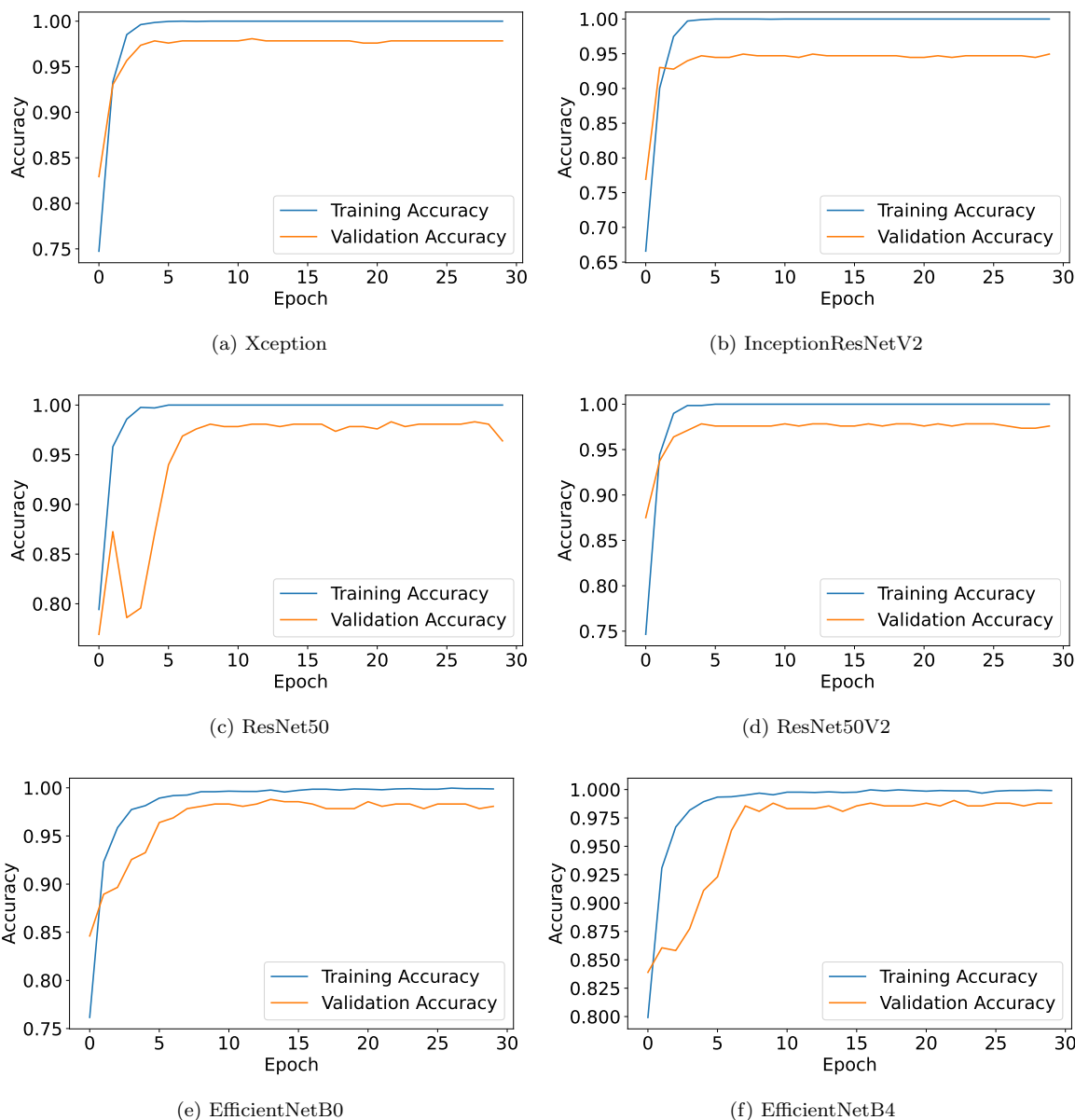


Figure 12: Accuracy Graph of DL models

Figure 12 depicts the training and validation accuracy during the experiments. The Y-axis represents the learning accuracy and X-axis represents the experiences for any algorithms. As we can see, with the increasing order of the epoch over time increases the training and validation accuracy. For any case, the training accuracy after 5 epochs and remains constant and validation accuracy reaches a steady state after 15 epochs. As a result, the curves demonstrate a satisfactory level of fitting for every model under consideration, both during the training phase and the validation test.

The time-varying loss curve for the training and validation sets is shown in Figure 13. The loss of the models

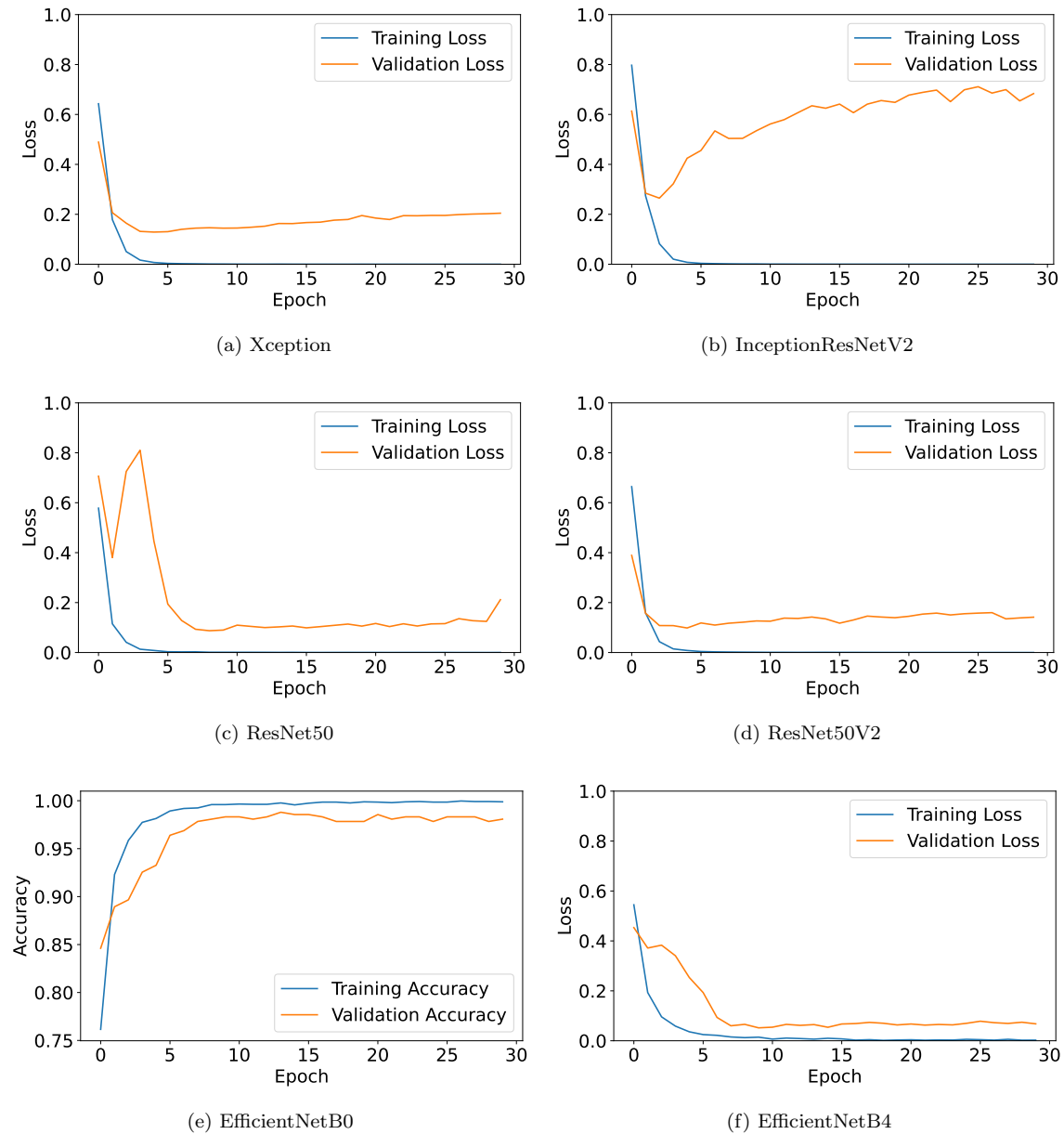


Figure 13: Loss Graph of DL models

decreases and stays closer to the training loss, demonstrating well-fitting characteristics, as shown by the graphs. While the validation loss was initially higher for ResNet50 and EfficientNetB4 up to epoch 15, it eventually leveled off and moved closer to the training loss, which displays the best-fit curves.

Among the evaluated models, EfficientNetB4 stands out as the indisputable best performer. Achieving perfect scores across all performance metrics, including accuracy, precision, recall, and F1-score, showcases unparalleled accuracy in detecting Lung disease as well as COVID-19 cases from medical images. Notably, EfficientNetB4 also demonstrates zero prediction error, making it an exceptional choice for real-world application. This model's outstanding performance signals its potential to revolutionize medical diagnostics and contribute significantly to global efforts in managing and mitigating the ongoing pandemic.

5.2.1. Discussion

The discussion section delves into the performance analysis of different deep learning models fine-tuned for Lung disease detection using the Chest X-Ray dataset illustrated in Table 7. The models evaluated include Xception, InceptionResNetV2, ResNet50, ResNet50V2, EfficientNetB0, and EfficientNetB4, each of which underwent fine-tuning to enhance their suitability for COVID-19 detection. The dataset comprised 4,350 Chest X-Ray Images, and the primary performance metric, accuracy in percentage, was used to assess the models' effectiveness.

The performance results reveal noteworthy achievements across the models. Among the evaluated models, EfficientNetB4 stood out, achieving a remarkable accuracy score of 99.17%, thereby exhibiting the potential for highly accurate Lung disease and COVID-19 detection. Following closely, Xception also demonstrated commendable performance, achieving an accuracy of 98.75%, underlining their effectiveness in distinguishing Lung and COVID-19 cases from X-ray images. EfficientNetB0 and ResNet50V2 both achieved 98.33% accuracy and InceptionResNetV2 achieved accuracy scores of 97.32% as well as ResNet50 performed accuracy scores of 97.32%. These scores, while slightly lower than the top-performing models, still demonstrate a high degree of accuracy in lung and COVID-19 detection using X-ray images.

The outcomes affirm that fine-tuning deep learning models significantly contributes to their diagnostic capabilities for Lung disease. The high accuracy achieved by various models indicates their potential to serve as reliable tools for medical practitioners in identifying lung and COVID-19 cases through X-ray images. The variations in accuracy scores between models emphasize the importance of selecting an appropriate architecture for a specific diagnostic task.

It is important to acknowledge that the presented accuracy scores represent real-world scenarios of collected data. Nevertheless, the results provide valuable insight into the capabilities of different DL models for Lung and COVID-19 detection from X-ray images. Among all, EfficientnetB4 provides comprehensive better results than others, which can help in aiding the development of accurate and reliable diagnostic tools for effective pandemic management.

Model	Method	Dataset	No. of Images	Performance (Accuracy in %)
Xception	Xception + Fine-Tuning	Chest X-Ray	4350	98.75
InceptionResNetV2	InceptionResNetV2 + Fine-Tuning	Chest X-Ray	4350	96.67
ResNet50	ResNet50 + Fine-Tuning	Chest X-Ray	4350	96.88
ResNet50V2	ResNet50V2 + Fine-Tuning	Chest X-Ray	4350	98.33
EfficientNetB0	EfficientNetB0 + Fine-Tuning	Chest X-Ray	4350	98.33
Proposed (EfficientNetB4)	EfficientNetB4 + Fine-Tuning	Chest X-Ray	4350	99.17

Table 7: Comparison analysis of proposed Fine-Tuned DL model with others on COVID-19 Data

The exploration of solutions to address the aforementioned concerns involves proposing methodologies for the following inquiries: Firstly, how to formulate an optimal automated COVID detection model that not only enhances accuracy but also effectively tackles the limitations evident in current solutions. Secondly, how to seamlessly integrate this novel detection model with Lung and COVID-19 X-Ray datasets, ensuring harmonious compatibility to capitalize on its potential for achieving precise predictions. Lastly, how to fine-tune and optimize existing models

to attain significantly heightened levels of accuracy, thereby reinforcing the reliability and efficacy of Lung and COVID-19 detection mechanisms.

5.2.2. Complexity Analysis

The complexity analysis of the prediction table revolves around the interplay between prediction speed and model accuracy in various DL models. In this context, complexity refers to the balance between computational efficiency and predictive capability. Table 5 presents prediction speeds, measured in seconds per prediction, as indicators of computational efficiency. Notably, ResNet50 emerges as the quickest, requiring just 32 seconds. Xception, EfficientNetB0 and ResNet50V2 share a marginally slower speed at 33, 34 and 35 seconds, respectively. InceptionResNetV2 takes much more than others, which is 50 seconds and the Proposed (EfficientNetB4) model demands 41 seconds for a prediction, marking them as the slowest. The note about the proposed EfficientNetB4 model adds an accuracy dimension to the analysis. Although it takes a bit more seconds in prediction, it promises the highest accuracy. This illustrates the inherent trade-off: higher accuracy often necessitates more complex models, prolonging prediction times. In practice, choosing a model entails considering trade-offs. For tasks valuing precision over real-time response, EfficientNetB4 could excel. Conversely, time-sensitive applications might favor quicker models like Xception, compromising some accuracy. The analysis underscores the delicate balance between prediction speed, accuracy, and model complexity. This understanding empowers decision-makers to select models aligning with specific needs, optimizing the intricate relationship between computational efficiency and predictive performance.

Proposed Model	Prediction Speed (In sec)
Xception	33
InceptionResNetV2	50
ResNet50	32
ResNet50V2	35
EfficientNetB0	34
EfficientNetB4	41

Table 8: Prediction Speeds of Different DL Models

6. Conclusions

In this study, we embarked on a comprehensive exploration of Lung and COVID-19 detection through the application of image preprocessing techniques coupled with various transfer learning models using modified architecture as well as fine-tuned the models for our proposal. Our extensive experimentation spanned diverse datasets to extract optimal performance for Lung and COVID-19 identification. Notably, our findings underscored the remarkable performance of the EfficientNetB4 algorithm in distinguishing Lung and COVID-19 manifestations from normal images, surpassing the efficacy of Xception, InceptionResNetV2, ResNet50, ResNet50V2, EfficientNetB0 and EfficientNetB4.

Our results established the supremacy of EfficientNetB4 in identifying COVID-19 X-ray images and showcased its exceptional performance with a high-scored ensemble of metrics. The proposed fine-tuned transfer learning model exhibited an impressive accuracy rate of 100%, precision, recall, and f1-score rates of 100%, alongside minimal MAE, MSE, and RMSE rates, all attesting to its robust diagnostic prowess. These findings emphasize the potential of fine-tuned transfer learning to expedite and economize COVID-19 detection through medical imaging, especially when X-ray images are available.

Moreover, the Lung disease detection experiment established on the Chest X-Ray Image dataset, the supremacy of EfficientNetB4 in identifying Lung X-ray images and showcased its exceptional performance with a high-scored ensemble of metrics. The proposed fine-tuned transfer learning model exhibited an impressive accuracy rate of 99.17%, precision of 99.13%, recall of 99.16%, and f1-score rates of 99.14%, alongside minimal MAE, MSE, and RMSE rates of 1.12%, 2.08% 14.43% respectively, all attesting to its robust diagnostic prowess. These findings emphasize the potential of fine-tuned transfer learning to expedite and economize Lung detection through medical imaging, especially using X-ray images.

However, this research venture opens avenues for future exploration. Further investigations could incorporate feature extraction and selection strategies into transfer learning paradigms, integrating deep learning with machine learning models and harnessing attention-based deep learning algorithms to enhance COVID-19 prediction accuracy. Additionally, expanding our analysis to encompass a larger repository of multi-class MRI and CT scan images from Bangladeshi patients is envisaged to bolster the precision of our approach. The implications of our work extend to radiological and clinical realms, potentially furnishing medical professionals with valuable diagnostic tools. As the field of medical imaging continues to evolve, our research stands as a testament to the potential synergy between advanced neural network architectures and healthcare diagnostics.

CRedit authorship contribution statement

Md. Alamin Talukder: Conceptualization, Data curation, Methodology, Software, Visualization, Analysis, Writing–original draft and review & editing. Md. Abu Layek: Analysis, Visualization, Investigation. Mohsin Kazi: Supervision, Analysis, Visualization, Writing–review & editing. Md Ashraf Uddin: Visualization, Investigation, Writing–review & editing Sunil Aryal: Visualization, Investigation.

Declaration of competing interest

The authors declare that they have no known competing financial interests or personal relationships that could have appeared to influence the work reported in this paper.

Acknowledgments

The authors would like to extend their sincere appreciation to the Researchers Supporting Project Number (RSP2023R301), King Saud University, Riyadh, Saudi Arabia.

References

- Aff, M., Ayachi, R., Said, Y., and Atri, M. (2023). Deep learning-based technique for lesions segmentation in ct scan images for covid-19 prediction. *Multimedia Tools and Applications*, pages 1–15.
- Agrawal, S., Honnakasturi, V., Nara, M., and Patil, N. (2023). Utilizing deep learning models and transfer learning for covid-19 detection from x-ray images. *SN Computer Science*, 4(4):326.
- Ahamed, K. U., Islam, M., Uddin, A., Akhter, A., Paul, B. K., Yousuf, M. A., Uddin, S., Quinn, J. M., and Moni, M. A. (2021). A deep learning approach using effective preprocessing techniques to detect covid-19 from chest ct-scan and x-ray images. *Computers in biology and medicine*, 139:105014.
- Ahamed, M. K. U., Islam, M. M., Uddin, M. A., Akhter, A., Acharjee, U. K., Paul, B. K., and Moni, M. A. (2023). Dtlcx: An improved resnet architecture to classify normal and conventional pneumonia cases from covid-19 instances with grad-cam-based superimposed visualization utilizing chest x-ray images. *Diagnostics*, 13(3):551.
- Ahmed, W., Simpson, S. L., Bertsch, P. M., Bibby, K., Bivins, A., Blackall, L. L., Bofill-Mas, S., Bosch, A., Brandão, J., Choi, P. M., et al. (2022). Minimizing errors in rt-pcr detection and quantification of sars-cov-2 rna for wastewater surveillance. *Science of the Total Environment*, 805:149877.
- Alamri, S. S., Alsaieedi, A., Khouqeer, Y., Afeef, M., Alharbi, S., Algaissi, A., Alghanmi, M., Altorki, T., Zawawi, A., Alfaleh, M. A., et al. (2023). The importance of combining serological testing with rt-pcr assays for efficient detection of covid-19 and higher diagnostic accuracy. *PeerJ*, 11:e15024.
- Asif, S., Wenhui, Y., Amjad, K., Jin, H., Tao, Y., and Jinhai, S. (2023). Detection of covid-19 from chest x-ray images: Boosting the performance with convolutional neural network and transfer learning. *Expert Systems*, 40(1):e13099.
- Batagelj, B., Peer, P., Štruc, V., and Dobrišek, S. (2021). How to correctly detect face-masks for covid-19 from visual information? *Applied Sciences*, 11(5):2070.
- Brooks, Z. C. and Das, S. (2020). Covid-19 testing: impact of prevalence, sensitivity, and specificity on patient risk and cost. *American Journal of Clinical Pathology*, 154(5):575–584.
- Chollet, F. (2017). Xception: Deep learning with depthwise separable convolutions. In *Proceedings of the IEEE conference on computer vision and pattern recognition*, pages 1251–1258.
- Choudhary, T., Gujar, S., Goswami, A., Mishra, V., and Badal, T. (2023). Deep learning-based important weights-only transfer learning approach for covid-19 ct-scan classification. *Applied Intelligence*, 53(6):7201–7215.
- Chowdhury, M. E., Rahman, T., Khandakar, A., Mazhar, R., Kadir, M. A., Mahbub, Z. B., Islam, K. R., Khan, M. S., Iqbal, A., Al Emadi, N., et al. (2020). Can ai help in screening viral and covid-19 pneumonia? *IEEE Access*, 8:132665–132676.

- Duong, L. T., Nguyen, P. T., Iovino, L., and Flammini, M. (2023). Automatic detection of covid-19 from chest x-ray and lung computed tomography images using deep neural networks and transfer learning. *Applied Soft Computing*, 132:109851.
- Elbeltagi, R., Al-Beltagi, M., Saeed, N. K., and Bediwy, A. S. (2023). Covid-19-induced gastrointestinal autonomic dysfunction: A systematic review. *World Journal of Clinical Cases*, 11(22):5246–5266.
- Eyiokur, F. I., Kantarcı, A., Erakın, M. E., Damer, N., Ofli, F., Imran, M., Krizaj, J., Salah, A. A., Waibel, A., Štruc, V., et al. (2022). A survey on computer vision based human analysis in the covid-19 era. *Image and Vision Computing*, page 104610.
- Filfilan, N. N., Bukhari, S., Rizwan, M., Bukhari, N. M., Aref, N. K., Arain, F. R., Alabbadi, I. K., Filfilan, N., BUKHARI, S., Albezrah, N., et al. (2023). Effects of different types of covid-19 vaccines on menstrual cycles of females of reproductive age group (15-49): A multinational cross-sectional study. *Cureus*, 15(5).
- He, K., Zhang, X., Ren, S., and Sun, J. (2016a). Deep residual learning for image recognition. In *Proceedings of the IEEE conference on computer vision and pattern recognition*, pages 770–778.
- He, K., Zhang, X., Ren, S., and Sun, J. (2016b). Identity mappings in deep residual networks. In *European conference on computer vision*, pages 630–645. Springer.
- Hemdan, E. E.-D., Shouman, M. A., and Karar, M. E. (2020). Covidx-net: A framework of deep learning classifiers to diagnose covid-19 in x-ray images. *arXiv preprint arXiv:2003.11055*.
- Islam, M. M., Talukder, M. A., Sarker, M. R. A., Uddin, M. A., Akhter, A., Sharmin, S., Al Mamun, M. S., and Debnath, S. K. (2023). A deep learning model for cotton disease prediction using fine-tuning with smart web application in agriculture. *Intelligent Systems with Applications*, 20:200278.
- Karakanis, S. and Leontidis, G. (2021). Lightweight deep learning models for detecting covid-19 from chest x-ray images. *Computers in biology and medicine*, 130:104181.
- Kathamuthu, N. D., Subramaniam, S., Le, Q. H., Muthusamy, S., Panchal, H., Sundararajan, S. C. M., Alrubaie, A. J., and Zahra, M. M. A. (2023). A deep transfer learning-based convolution neural network model for covid-19 detection using computed tomography scan images for medical applications. *Advances in Engineering Software*, 175:103317.
- Kogilavani, S., Prabhu, J., Sandhiya, R., Kumar, M. S., Subramaniam, U., Karthick, A., Muhibbullah, M., and Imam, S. B. S. (2022). Covid-19 detection based on lung ct scan using deep learning techniques. *Computational and Mathematical Methods in Medicine*, 2022.
- Kumar, N., Gupta, M., Gupta, D., and Tiwari, S. (2023). Novel deep transfer learning model for covid-19 patient detection using x-ray chest images. *Journal of ambient intelligence and humanized computing*, 14(1):469–478.
- Kumar, S. and Mallik, A. (2023). Covid-19 detection from chest x-rays using trained output based transfer learning approach. *Neural processing letters*, 55(3):2405–2428.

- Li, D., Sun, C., Zhuang, P., and Mei, X. (2023a). Revolutionizing sars-cov-2 omicron variant detection: Towards faster and more reliable methods. *Talanta*, page 124937.
- Li, G., Togo, R., Ogawa, T., and Haseyama, M. (2023b). Covid-19 detection based on self-supervised transfer learning using chest x-ray images. *International Journal of Computer Assisted Radiology and Surgery*, 18(4):715–722.
- Madhavan, M. V., Khamparia, A., Gupta, D., Pande, S., Tiwari, P., and Hossain, M. S. (2023). Res-covnet: An internet of medical health things driven covid-19 framework using transfer learning. *Neural Computing and Applications*, 35(19):13907–13920.
- Motta, P. C., Cesar Cortez, P., and Lobo Marques, J. A. (2023). Covid-19 classification using ct scans with convolutional neural networks. In *Computerized Systems for Diagnosis and Treatment of COVID-19*, pages 99–116. Springer.
- Muhammad, U., Hoque, M. Z., Oussalah, M., Keskinarkaus, A., Seppänen, T., and Sarder, P. (2022). Sam: Self-augmentation mechanism for covid-19 detection using chest x-ray images. *Knowledge-Based Systems*, 241:108207.
- Nemati, M., Jafari, A., Ebrahimi, Y., Golchin, A., Pouya, F. D., Rezaei-Tavirani, M., and Rasmi, Y. (2023). Laboratory methods: A concise review and update for covid-19 diagnosis. *Cell Biochemistry and Function*.
- Nigam, B., Nigam, A., Jain, R., Dodia, S., Arora, N., and Annappa, B. (2021). Covid-19: Automatic detection from x-ray images by utilizing deep learning methods. *Expert Systems with Applications*, 176:114883.
- Panwar, H., Gupta, P., Siddiqui, M. K., Morales-Menendez, R., and Singh, V. (2020). Application of deep learning for fast detection of covid-19 in x-rays using ncovnet. *Chaos, Solitons & Fractals*, 138:109944.
- Peeling, R. W., Wedderburn, C. J., Garcia, P. J., Boeras, D., Fongwen, N., Nkengasong, J., Sall, A., Tanuri, A., and Heymann, D. L. (2020). Serology testing in the covid-19 pandemic response. *The Lancet Infectious Diseases*, 20(9):e245–e249.
- Rahimzadeh, M. and Attar, A. (2020). A modified deep convolutional neural network for detecting covid-19 and pneumonia from chest x-ray images based on the concatenation of xception and resnet50v2. *Informatics in medicine unlocked*, 19:100360.
- Ramanna, S., Sengoz, C., Kehler, S., and Pham, D. (2021). Near real-time map building with multi-class image set labeling and classification of road conditions using convolutional neural networks. *Applied Artificial Intelligence*, 35(11):803–833.
- Rana, M. M., Islam, M. M., Talukder, M. A., Uddin, M. A., Aryal, S., Alotaibi, N., Alyami, S. A., Hasan, K. F., and Moni, M. A. (2023). A robust and clinically applicable deep learning model for early detection of alzheimer’s. *IET Image Processing*, pages 1–17.
- Reddy, A. S. B. and Juliet, D. S. (2019). Transfer learning with resnet-50 for malaria cell-image classification. In *2019 International Conference on Communication and Signal Processing (ICCSP)*, pages 0945–0949. IEEE.

- Reddy, A. S. K., Rao, K. B., Soora, N. R., Shailaja, K., Kumar, N. S., Sridharan, A., and Uthayakumar, J. (2023). Multi-modal fusion of deep transfer learning based covid-19 diagnosis and classification using chest x-ray images. *Multimedia Tools and Applications*, 82(8):12653–12677.
- Sarp, S., Catak, F. O., Kuzlu, M., Cali, U., Kusetogullari, H., Zhao, Y., Ates, G., and Guler, O. (2023). An xai approach for covid-19 detection using transfer learning with x-ray images. *Heliyon*, 9(4).
- Sharmin, S., Ahammad, T., Talukder, M. A., and Ghose, P. (2023). A hybrid dependable deep feature extraction and ensemble-based machine learning approach for breast cancer detection. *IEEE Access*.
- SUBASI, A., KELES, T., OZYURT, F., DOGAN, S., and TUNCER, T. (2023). Feature extraction and fusion using deep convolutional neural networks for covid-19 detection using ct and x-ray images. *World Journal of Advanced Research and Reviews*, 19(1):914–933.
- Subramanian, M., Sathishkumar, V. E., Cho, J., and Shanmugavadivel, K. (2023). Learning without forgetting by leveraging transfer learning for detecting covid-19 infection from ct images. *Scientific Reports*, 13(1):8516.
- Szegedy, C., Ioffe, S., Vanhoucke, V., and Alemi, A. A. (2017). Inception-v4, inception-resnet and the impact of residual connections on learning. In *Thirty-first AAAI conference on artificial intelligence*.
- Talukder, M. A. (2023). Chest x-ray image. Mendeley Data, V1.
- Talukder, M. A., Hasan, K. F., Islam, M. M., Uddin, M. A., Akhter, A., Yousuf, M. A., Alharbi, F., and Moni, M. A. (2023a). A dependable hybrid machine learning model for network intrusion detection. *Journal of Information Security and Applications*, 72:103405.
- Talukder, M. A., Islam, M. M., Uddin, M. A., and Akhter, A. (2022a). Covid19 xray data. Mendeley Data, V1.
- Talukder, M. A., Islam, M. M., Uddin, M. A., Akhter, A., Hasan, K. F., and Moni, M. A. (2022b). Machine learning-based lung and colon cancer detection using deep feature extraction and ensemble learning. *Expert Systems with Applications*, 205:117695.
- Talukder, M. A., Islam, M. M., Uddin, M. A., Akhter, A., Pramanik, M. A. J., Aryal, S., Almoyad, M. A. A., Hasan, K. F., and Moni, M. A. (2023b). An efficient deep learning model to categorize brain tumor using reconstruction and fine-tuning. *Expert Systems with Applications*, page 120534.
- Tan, M., Chen, B., Pang, R., Vasudevan, V., Sandler, M., Howard, A., and Le, Q. V. (2019). Mnasnet: Platform-aware neural architecture search for mobile. In *Proceedings of the IEEE/CVF Conference on Computer Vision and Pattern Recognition*, pages 2820–2828.
- Tan, M. and Le, Q. (2019). Efficientnet: Rethinking model scaling for convolutional neural networks. In *International conference on machine learning*, pages 6105–6114. PMLR.
- Tsang, S. (2018). Review: Xception-with depthwise separable convolution, better than inception-v3 (image classification). *Towards Data Science*, 25.

- Xue, X., Chinnaperumal, S., Abdulsahib, G. M., Manyam, R. R., Marappan, R., Raju, S. K., and Khalaf, O. I. (2023). Design and analysis of a deep learning ensemble framework model for the detection of covid-19 and pneumonia using large-scale ct scan and x-ray image datasets. *Bioengineering*, 10(3):363.
- Zheng, K., Wu, J., Yuan, Y., and Liu, L. (2023). From single to multiple: Generalized detection of covid-19 under limited classes samples. *Computers in Biology and Medicine*, page 107298.
- Zysman, M., Asselineau, J., Saut, O., Frison, E., Oranger, M., Maurac, A., Charriot, J., Achkir, R., Regueme, S., Klein, E., et al. (2023). Development and external validation of a prediction model for the transition from mild to moderate or severe form of covid-19. *European Radiology*, pages 1–13.